WNTEIPGITLVTEDIALPLMKVLSFKGYWEKLNSNLEYVK YAKPHFHYNNSVVRREWHNLISEE (1:100, HPA023994; Sigma). After washing with PBS, the tissue sections were labelled at RT for 30 min with peroxidase-conjugated secondary antibodies (Nichirei, Tokyo, Japan), followed by incubation with diaminobenzidine tetrahydrochloride (DAB) substrate and a DAB-enhancing solution (Vector, Burlingame, CA, USA). They were processed for a counterstain with haematoxylin. For negative controls, the primary antibody was preabsorbed with recombinant human GSAP protein tagged with Xpress produced by an *Escherichia coli* (*E. coli*) expression system.

For double-labelling immunohistochemistry, tissue sections were initially stained with mouse anti-PS1 monoclonal antibody (1:100, sc-80297; Santa Cruz Biotechnology, Santa Cruz, CA, USA), mouse anti-Aβ11-28 monoclonal antibody (1:50, 12B2; Immunobiological Laboratory, Gunma, Japan) or mouse anti-paired helical filament-tau monoclonal antibody (1:100, AT8; Thermo Scientific, Rockford, IL, USA), then followed by incubation with alkaline phosphatase-conjugated secondary antibody (Nichirei), and colourized with New Fuchsin substrate (Nichirei). After inactivation of the antibody by autoclaving the sections, they were relabelled with anti-GSAP antibody HPA020058, followed by incubation with peroxidase-conjugated secondary antibody, and colourized with DAB substrate.

Quantification of GSAP-immunoreactive particles

To quantify the number of GSAP-immunoreactive dot-like deposits, the images of three fields intervening between the hippocampal CA2 and CA3 regions at a ×200 magnification under microscope were captured, and processed for quantification of the particle signals with ImageJ software (National Institute of Health, Bethesda, MD, USA). The statistical difference in the average of counts/field between AD and non-AD groups was evaluated by Student's *t*-test.

Results

GSAP immunoreactivity exhibited four distinct morphological features

By immunohistochemistry using the antibody HPA020058, we identified GSAP immunoreactivity in both AD and non-AD brains. The specificity of the antibody was validated by Western blot of the corresponding recombinant protein fragment expressed in HEK293 cells and *E. coli* (Figure S1**a,b,d** and Figure S2**a**). Overall, the distribution of GSAP did not show apparent similarities to the pattern of expression of glial fibrillary acidic protein, Aβ or tau (Figure 1). In AD and control brains, GSAP-immunoreactive deposits were distributed chiefly in the neuropil and neuronal processes, and occasionally in neuronal cell bodies, vascular walls and perivascular cells. We categorized the morphology of GSAP-immunoreactive deposits into the following four patterns: (i) fine granular deposits located in the cytoplasm of a fairly small subset of cerebral cortical and hippocampal neurones in AD and control brains (Figure 2**a** and Figure 3**d**); (ii) dense nodular and patchy deposits, often being extracellular and forming clusters and clumps, located in the neuropil most frequently identified in AD brains but barely detectable in control brains (Figure 2**b–e**); (iii) beads and string-like deposits located in neuronal processes found in the cortex and the white matter of both AD and control brains (Figure 3**a,b**); and (iv) diffuse dot-like deposits located in the neuropil and neuronal processes, most frequently found in the hippocampal CA2 and CA3 regions of both AD and controls (Figure 3**c**). Thus, we found that dense nodular and patchy deposits located in the neuropil represent the most distinguishing characteristics of AD pathology, because this pattern was hardly found in control brains. The negative controls without inclusion of the primary antibody generated no discernible signals, and the antibody preabsorbed by recombinant GSAP protein produced greatly diminished signals (Figure S2, **c** *vs.* **b**). In contrast to detection of GSAP by immunohistochemistry, we could not detect GSAP expression by Western blot of sodium dodecyl sulphate-soluble protein extract isolated from the frontal cortex of AD and non-AD cases (Figure S1**e**), suggesting the possibility that the amounts of GSAP protein in the frontal cortex are below the detection level for Western blot by the antibody HPA020058, or alternatively that GSAP is sequestered in detergent-insoluble fractions *in vivo*.

The number of GSAP-immunoreactive dot-like deposits varied greatly among the cases

Because GSAP-immunoreactive dot-like deposits were commonly observed in both AD and control brains, we considered the possible scenario that dot-like deposits represent a predecessor of dense nodular and patchy deposits.

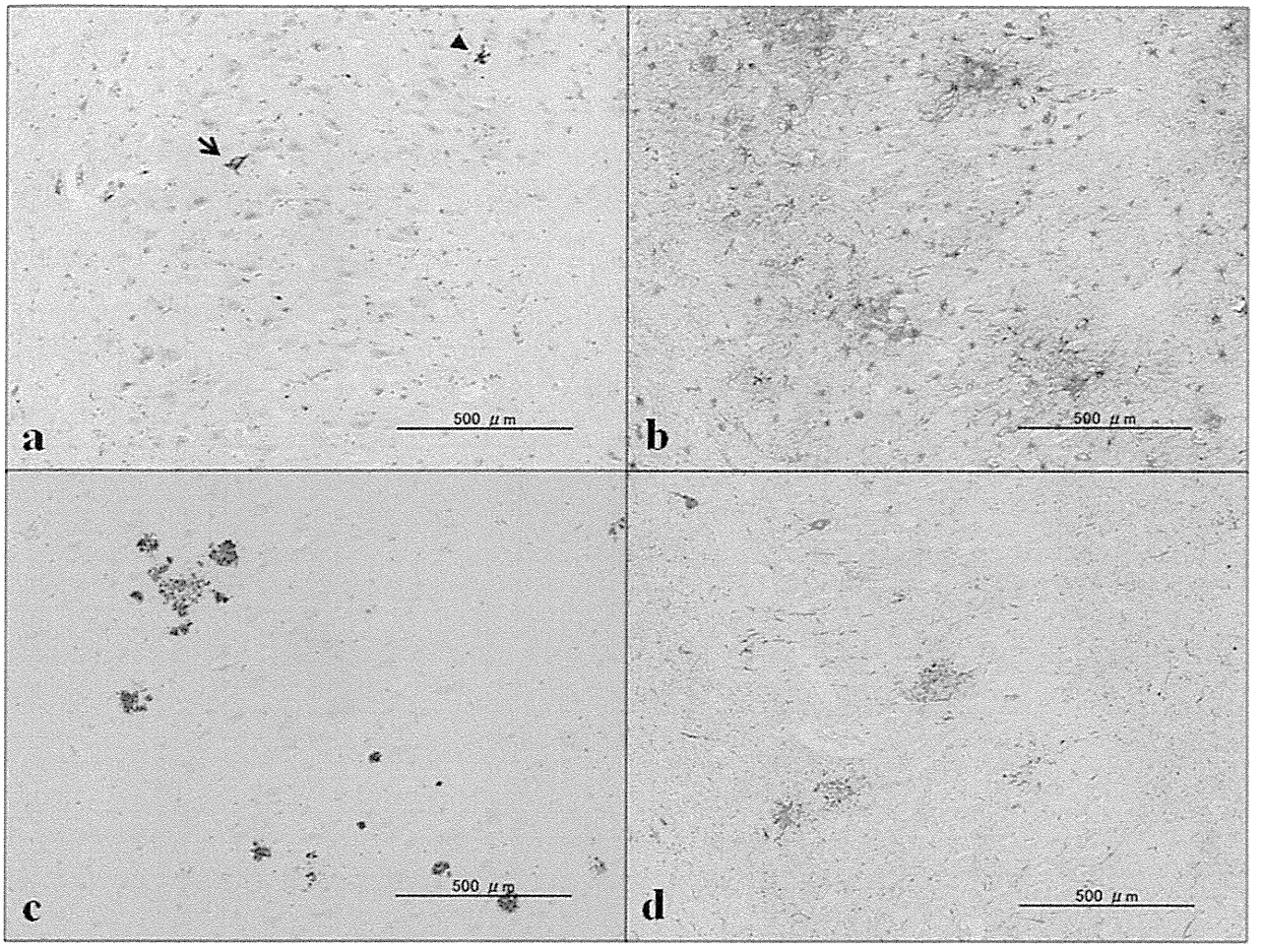

Figure 1. The expression of γ-secretase activating protein (GSAP), glial fibrillary acidic protein (GFAP), amyloid-β (Aβ) and tau in Alzheimer's disease (AD) brains. The panels (**a–d**) represent low magnification photographs of (**a**) GSAP (HPA020058), (**b**) GFAP, (**c**) Aβ and (**d**) tau (AT8) in serial tissue sections of the hippocampal CA3 region of AD. High magnification photographs corresponding to the region indicated by an arrow and an arrowhead in panel (**a**) are shown in Figure 2, panels **a** and **b**, respectively.

Therefore, we quantitatively evaluated the amount of dot-like particles in the hippocampal CA2 and CA3 regions by imaging them on ImageJ software. Contrary to our expectation, we found that the number of particles per field varied greatly among individual cases (Figure 4**a**). Although all AD cases examined in the present study are categorized into the most advanced stages of AD pathology, the number of GSAP-immunoreactive particles was surprisingly small in several AD cases, such as AD5, AD8, AD9 and AD11 (Figure 4**a**).

When the counts of dot-like deposits were compared between AD cases, all of which were categorized into the Braak NFT stage of VI ($n = 11$, the mean age of 71 ± 9 years) and non-AD cases categorized into the stages III/IV compatible with NFT pathology of the early AD ($n = 5$, the mean age of 64 ± 10 years), the difference did not become statistically significant ($P = 0.462$) (Figure 4**b**). However, when they were compared between AD cases and non-AD cases categorized into the stages II/III compatible with NFT pathology of normal ageing and the earliest AD ($n = 9$, the mean age of 74 ± 11 years), the difference became statistically significant ($P = 0.043$) (Figure 4**c**). When the counts of dot-like deposits were compared between the cases with almost no Aβ deposits classified as the stage Zero of amyloid deposition ($n = 8$, the mean age of 66 ± 7 years) and those with extensive Aβ deposits classified as the stage C of amyloid deposition ($n = 13$, the mean age of 71 ± 8 years), the difference did not become statistically significant ($P = 0.926$) (Figure 4**d**). These results suggest that there exists a trend

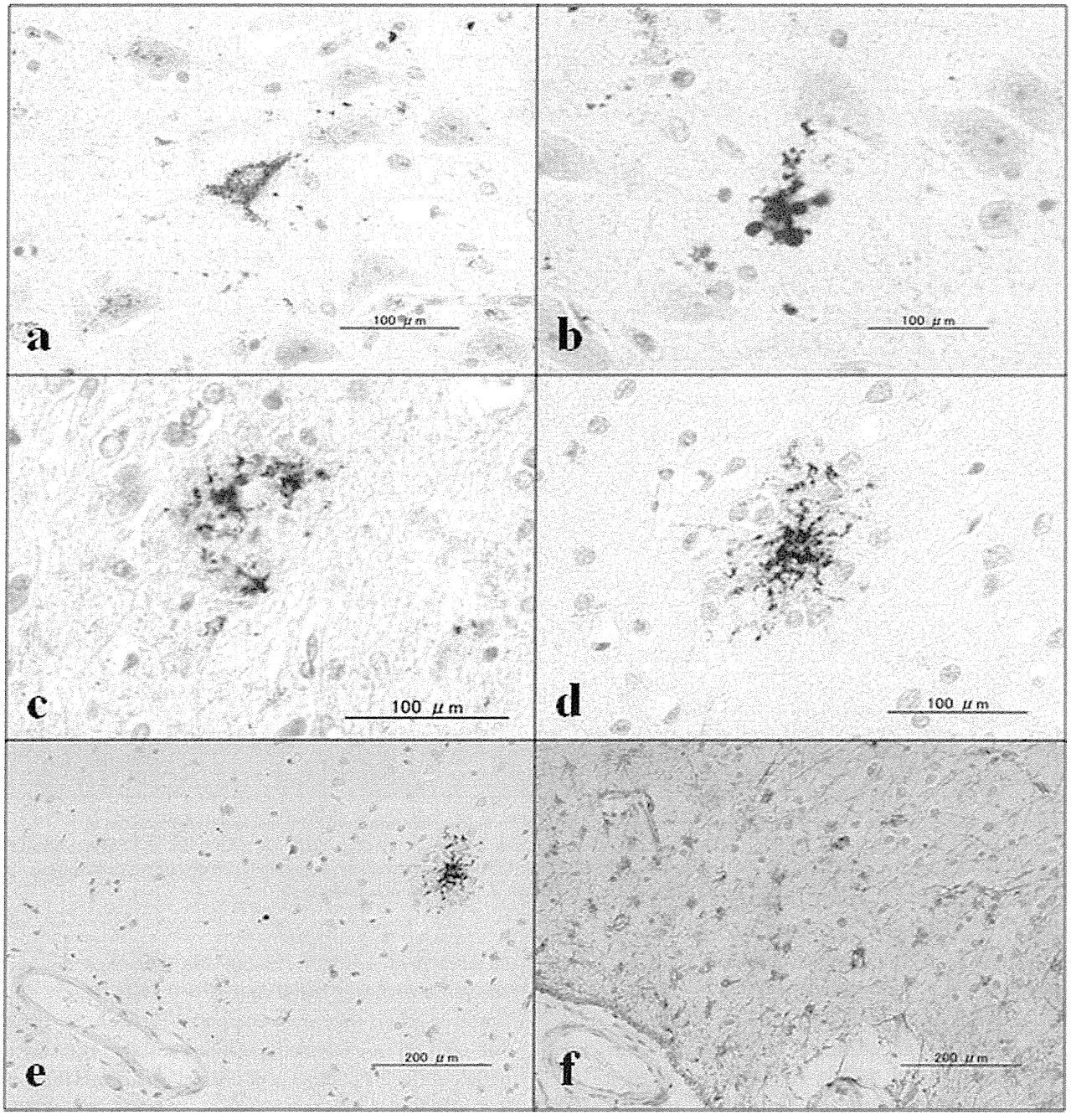

Figure 2. γ-Secretase activating protein (GSAP) expression in Alzheimer's disease (AD) brains. The panels (**a–f**) represent GSAP immunoreactivity of (**a**) fine granular deposits in the neuronal cytoplasm in the hippocampal CA3 region of AD, (**b**) a clump of dense nodular deposits in the neuropil in the hippocampal CA3 region of AD, (**c**) a cluster of dense patchy deposits in the neuropil in the frontal cortex of AD, (**d**) a clump of dense patchy deposits in the neuropil in the frontal cortex of AD, and low magnification photographs of (**e**) the region corresponding to (**d**), and (**f**) glial fibrillary acidic protein of the serial tissue section corresponding to (**e**).

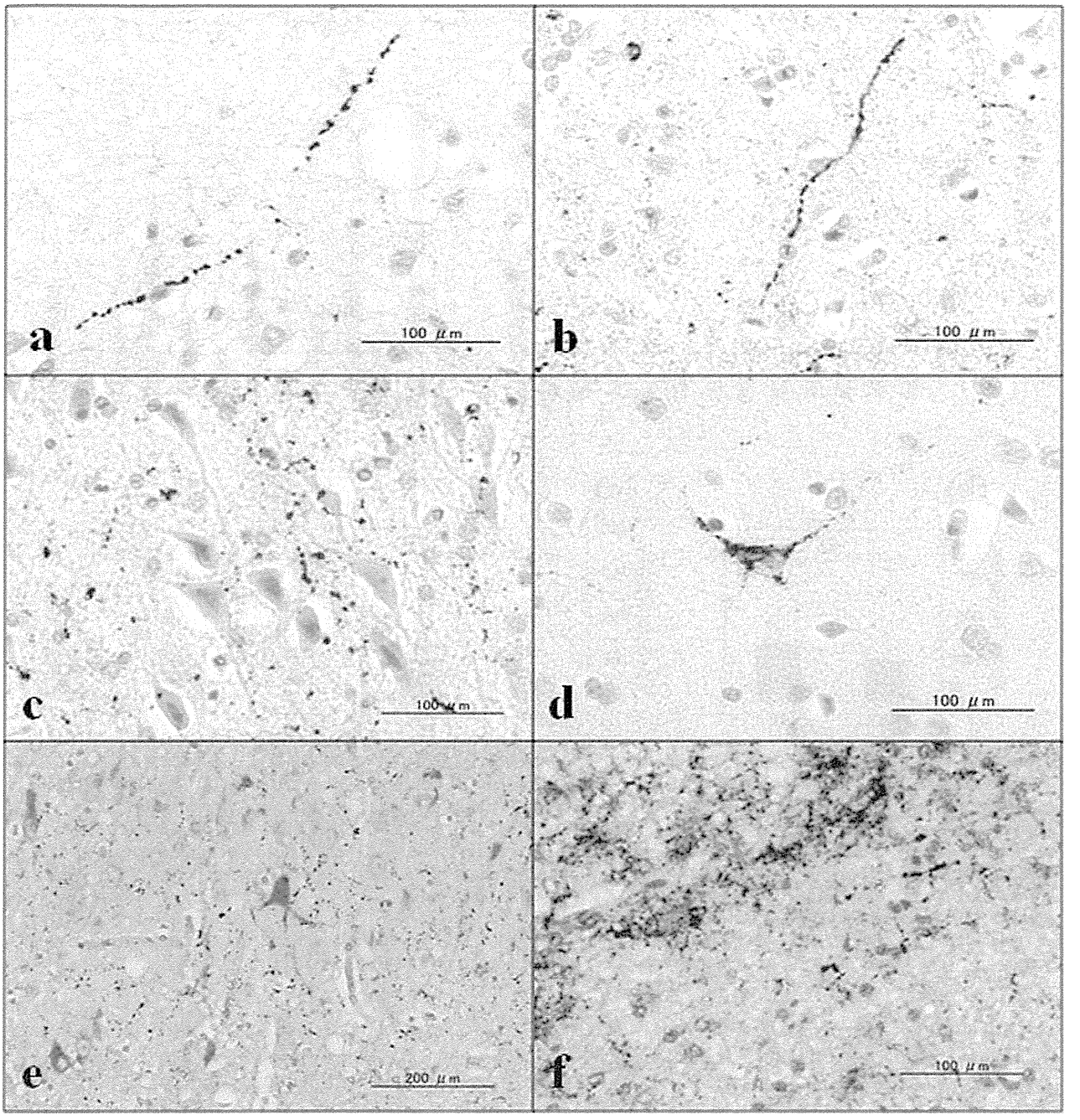

Figure 3. γ-Secretase activating protein (GSAP) expression in Alzheimer's disease (AD) and control brains. The panels (**a–d**) represent GSAP immunoreactivity of (**a**) beads and string-like deposits in neuronal processes in the frontal cortex of AD, (**b**) beads and string-like deposits in neuronal processes in the frontal cortex of myotonic dystrophy, (**c**) diffuse dot-like deposits in the neuropil and neuronal processes in the hippocampal CA3 region of amyotrophic lateral sclerosis (ALS), (**d**) fine granular deposits in the neuronal cytoplasm in the frontal cortex of normal control, (**e**) double labelling of tau (AT8; red) and GSAP (brown; diffuse dot-like deposits in the neuropil) in the hippocampal CA2 region of ALS, and (**f**) double labelling of tau (AT8; red) and GSAP (brown; diffuse dot-like deposits in the neuropil) in the hippocampal CA3 region of AD.

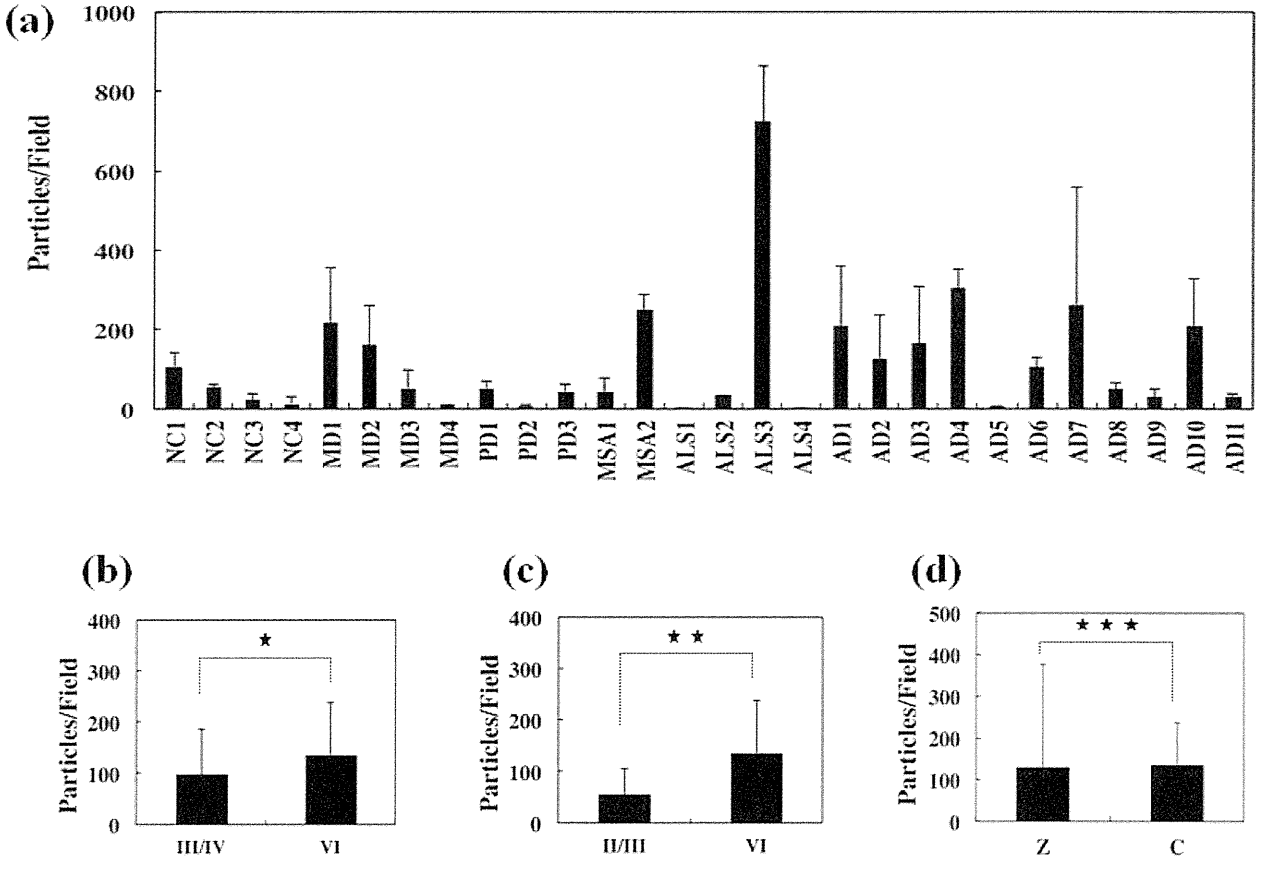

Figure 4. Quantification of γ-secretase activating protein (GSAP)-immunoreactive particles in the hippocampus of Alzheimer's disease (AD) and control brains. The number of diffuse dot-like deposits was counted by imaging of three fields of hippocampal CA2 and CA3 regions with ImageJ software. The panels (**a–c**) represent (**a**) the average of counts/field in individual case expressed as the bar with standard deviation, (**b**) the average of counts/field compared between AD cases categorized into the Braak stage VI ($n = 11$) and non-AD cases categorized into the stages III/IV ($n = 5$), (**c**) the average of counts/field compared between AD cases categorized into the stage VI ($n = 11$) and non-AD cases categorized into the stages II/III ($n = 9$), and (**d**) the average of counts/field compared between the cases with almost no amyloid-β (Aβ) deposits classified as the stage Zero (Z) of amyloid deposition ($n = 8$) and those with extensive Aβ deposits classified as the stage C of amyloid deposition ($n = 13$). The single star (panel **b**) indicates the statistical difference with $P = 0.462$; double stars (panel **c**) indicate the difference with $P = 0.043$; and triple stars (panel **d**) indicate the difference with $P = 0.926$. NC, normal control; MD, myotonic dystrophy; PD, Parkinson's disease; MSA, multiple system atrophy; ALS, amyotrophic lateral sclerosis.

towards accumulation of greater amounts of GSAP-immunoreactive particles in the hippocampus of more advanced stages of the disease defined by NFT irrespective of Aβ accumulation.

The close association of GSAP-immunoreactive deposits with PS1 and Aβ in AD brains

Finally, we investigated the association of GSAP-immunoreactive deposits with the potential interacting partner PS1 and the end-product Aβ. PS1 was intensely expressed and ubiquitously distributed in the neuronal cytoplasm and processes, and in addition, less intensely expressed in the neuropil, where GSAP-immunoreactive nodular, patchy and dot-like deposits were often in close contact with PS1 immunoreactivity (arrows in Figure 5**a,b**). Furthermore, GSAP-immunoreactive dense nodular, patchy and dot-like deposits were often located on the core and in the periphery of senile plaques that were labelled with Aβ (Figure 5**c–e**). In contrast, GSAP immunoreactivity was essentially differentiated from AT8-positive tau immunoreactivity (Figure 3**e,f**). The anti-PION non-GSAP antibody HPA023994 reacted with extremely small numbers of granular and nodular deposits (Figure 5**f**), indicating that the great majority of GSAP-immunoreactive deposits labelled with the anti-PION

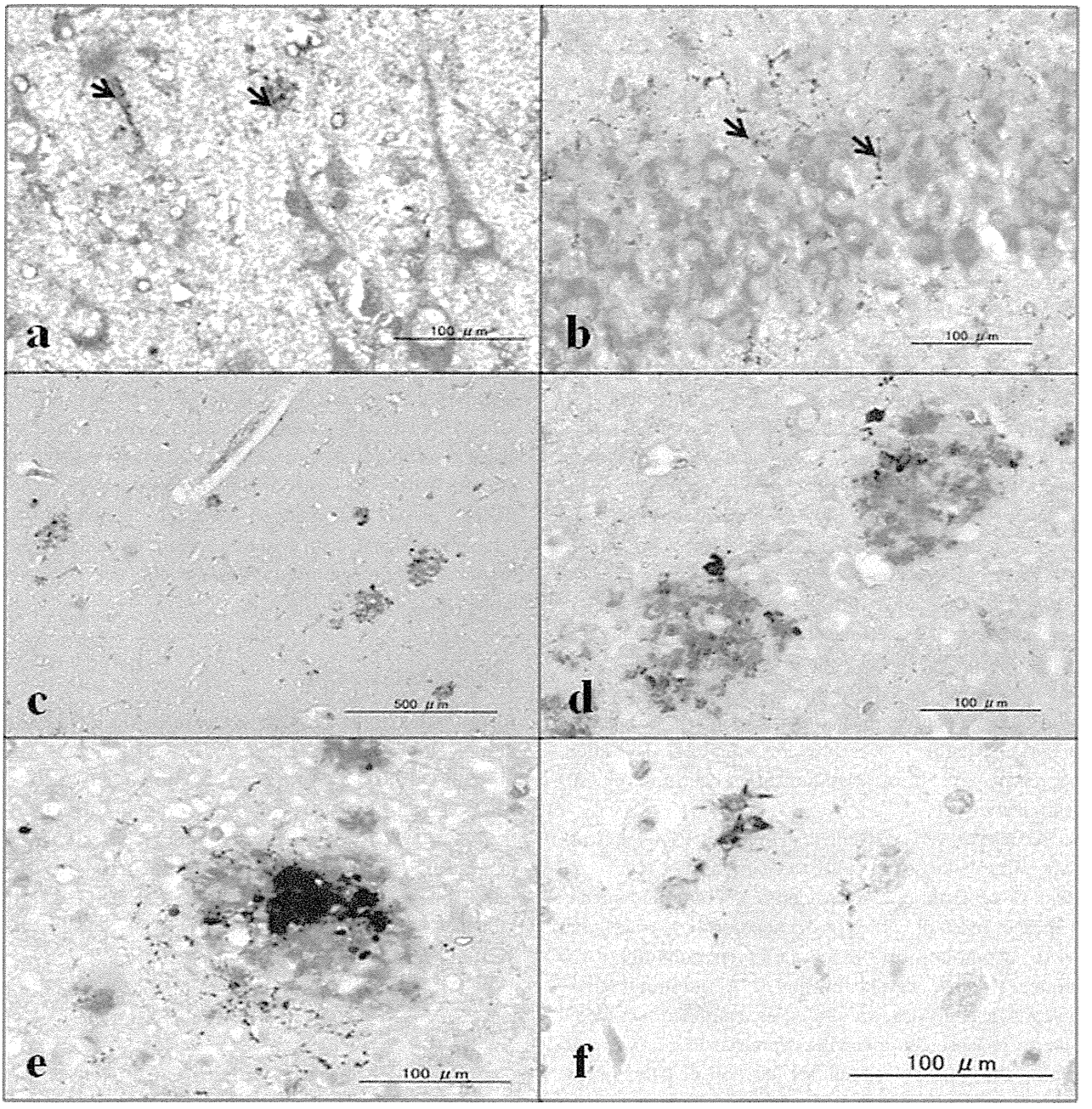

Figure 5. Close association of γ-secretase activating protein (GSAP) with presenilin-1 (PS1) and amyloid-β (Aβ). The panels (**a–f**) represent (**a**) double labelling of PS1 (red) and GSAP (brown; dot-like deposits in the neuronal processes and the neuropil) in the frontal cortex of Alzheimer's disease (AD) where the arrows indicate the close contact between GSAP and PS1, (**b**) double labelling of PS1 (red) and GSAP (brown; dot-like deposits in the neuropil) in the granule cell layer of the hippocampal dentate gyrus of AD where the arrows indicate the close contact between GSAP and PS1, (**c**) low magnification photograph of double labelling of Aβ (red) and GSAP (brown) in the frontal cortex of AD, (**d**) high magnification photograph of (**c**), (**e**) double labelling of Aβ (red) and GSAP (brown; a clump of dense nodular deposits and many dot-like deposits) in the frontal cortex of AD, and (**f**) PION immunoreactivity labelled with anti-PION non-GSAP antibody HPA023994 in the frontal cortex of AD.

antibody HPA020058 do not represent the full-length PION protein, but reflect the processed form of PION containing the C-terminal GSAP segment.

Discussion

γ-Secretase activating protein acts as a key molecule responsible for the rate-limiting step in Aβ production by interacting with PS1-CTF and the juxtamembrane region of APP-CTF [5]. Because GSAP modulates γ-cleavage of APP but not of Notch, it would serve as an ideal target molecule for designing γ-secretase modulators with least side effects for AD therapy [6]. Here we for the first time characterized GSAP expression in AD brains by immunohistochemistry. GSAP-immunoreactive deposits are located chiefly in the neuropil and neuronal processes, and occasionally in neuronal cytoplasm in the cerebral cortex and the hippocampus of both AD and control brains, indicating that it did not represent an AD-specific biomarker. GSAP-immunoreactive deposits exhibited four distinct morphological features, such as fine granular cytoplasmic deposits, dense nodular and patchy deposits, beads and string-like deposits, and diffuse dot-like deposits. Among them, dense nodular and patchy deposits, located in the neuropil and closely associated with PS1 expression and Aβ deposition, represent the most distinguishing features of AD pathology.

Because GSAP is concentrated in a trans-Golgi network when overexpressed in cultured cells [5], it is unexpected that GSAP-immunoreactive dense nodular and patchy deposits, most of which were apparently extracellular, were accumulated in the neuropil predominantly of AD brains. Because we did not find GSAP-immunoreactive intranuclear deposits in any cases examined, we would like to propose the following scenario. In normal neurones, the primary subcellular location of GSAP is the cytoplasm, including endoplasmic reticulum and Golgi, distributed widely in neuronal processes via axonal and dendritic transport. Under physiological conditions, a fine balance between production and turnover of GSAP maintains it at very low constitutive levels, resulting in no obvious accumulation of dense nodular and patchy GSAP deposits. By contrast, in degenerating neurones of AD brains, aberrant regulation of GSAP expression, processing, transport and turnover induces formation of intracellular and extracellular aggregates, which are potentially associated with acceleration of Aβ overproduction.

γ-Secretase activating protein is derived from a C-terminal fragment of PION via an unknown processing mechanism. By bioinformatics analysis, we found that PION exists in the genomes of *Homo sapiens* (Entrez Gene ID 54103), *Pan troglodytes* (472424), *Bos taurus* (615147), *Canis lupus familiaris* (475903), *Mus musclus* (212167), *Rattus norvegiucus* (311984), *Gallus gallus* (417724) and *Danio rerio* (100151358). Importantly, the GSAP fragment corresponding to amino acid residues of 733-854 of the human PION protein is highly conserved through evolution except for the rat. Although the rat PION mRNA sequence (NM_001107845.1) represents a provisional one, it is almost completely devoid of GSAP (Figure S3). These results suggest that GSAP plays an evolutionarily conserved role in a wide range of vertebrate species, although it is unlikely to be indispensable for mammalian brain development and maturation, when the lack of GSAP is validated in the rat. Detailed characterization of GSAP distribution in various animal cells and tissues is seemingly important to elucidate the conserved biological function of GSAP.

Acknowledgements

All autopsied brain samples were obtained from Research Resource Network (RRN), Japan. This work was supported by grants to J-IS from Research on Intractable Diseases (H21-Nanchi-Ippan-201 and H22-Nanchi-Ippan-136), the Ministry of Health, Labour and Welfare (MHLW), Japan, and the High-Tech Research Center Project (S0801043) and the Grant-in-Aid (C22500322), the Ministry of Education, Culture, Sports, Science and Technology (MEXT), Japan.

References

1 Selkoe DJ. Alzheimer's disease: genes, proteins, and therapy. *Physiol Rev* 2001; **81**: 741–66
2 De Strooper B, Annaert W. Novel research horizons for presenilins and γ-secretases in cell biology and disease. *Annu Rev Cell Dev Biol* 2010; **26**: 235–60
3 Wolfe MS. Inhibition and modulation of γ-secretase for Alzheimer's disease. *Neurotherapeutics* 2008; **5**: 391–8
4 Netzer WJ, Dou F, Cai D, Veach D, Jean S, Li Y, Bornmann WG, Clarkson B, Xu H, Greengard P. Gleevec inhibits β-amyloid production but not Notch cleavage. *Proc Natl Acad Sci U S A* 2003; **100**: 12444–9
5 He G, Luo W, Li P, Remmers C, Netzer WJ, Hendrick J, Bettayeb K, Flajolet M, Gorelick F, Wennogle LP, Greengard P. Gamma-secretase activating protein is a

therapeutic target for Alzheimer's disease. *Nature* 2010; **467**: 95–8
6 St George-Hyslop P, Schmitt-Ulms G. Alzheimer's disease: selectively tuning γ-secretase. *Nature* 2010; **467**: 36–7
7 Mirra SS, Gearing M, McKeel DW Jr, Crain BJ, Hughes JP, van Belle G, Heyman A. The Consortium to Establish a Registry for Alzheimer's Disease (CERAD). Part II. Standardization of the neuropathologic assessment of Alzheimer's disease. *Neurology* 1991; **41**: 479–86
8 Misawa T, Arima K, Mizusawa H, Satoh J. Close association of water channel AQP1 with amyloid-β deposition in Alzheimer disease brains. *Acta Neuropathol* 2008; **116**: 247–60
9 Satoh J, Tabunoki H, Arima K. Molecular network analysis suggests aberrant CREB-mediated gene regulation in the Alzheimer disease hippocampus. *Dis Markers* 2009; **27**: 239–52
10 Shioya M, Obayashi S, Tabunoki H, Arima K, Saito Y, Ishida T, Satoh J. Aberrant microRNA expression in the brains of neurodegenerative diseases: miR-29a decreased in Alzheimer disease brains targets neurone navigator 3. *Neuropathol Appl Neurobiol* 2010; **36**: 320–30
11 Braak H, Braak E. Neuropathological stageing of Alzheimer-related changes. *Acta Neuropathol* 1991; **82**: 239–59
12 Braak H, Alafuzoff I, Arzberger T, Kretzschmar H, Del Tredici K. Staging of Alzheimer disease-associated neurofibrillary pathology using paraffin sections and immunocytochemistry. *Acta Neuropathol* 2006; **112**: 389–404

Supporting information

Additional Supporting Information may be found in the online version of this article:

Figure S1. Western blot of γ-secretase activating protein (GSAP). The present study utilized a rabbit anti-GSAP antibody (HPA020058; Sigma, St. Louis, MO, USA) or a rabbit anti-PION non-GSAP fragment antibody (HPA023994; Sigma). The precise amino acid sequences of the antigens are specified in the *Materials and methods* section. The specificity of the antibodies was validated by Western blot of corresponding recombinant protein fragments tagged with V5 expressed in HEK293 cells. The panels (**a–f**) represent the blots of (**a**–left, **d**, **e**) HPA020058, (**a**–right) HPA023994, (**b**) V5, (**c**) heat shock protein 60, an internal control of protein loading, and (**f**) 14-3-3 (K-19), an internal control of protein loading. The lanes (1–12) represent (1, 3, 5) non-transfected cells, (2, 6) the cells transfected with the vector expressing GSAP covering amino acid residues 734-854, (4) the cells transfected with the vector expressing non-GSAP PION covering amino acid residues 427-567, and 80 μg sodium dodecyl sulphate-soluble protein extract isolated from the frontal cortex of (7) NC2, (8) NC3, (9) ALS2, (10) ALS3, (11) AD3 and (12) AD5. IgH indicates non-specific bands corresponding to the immunoglobulin heavy chain. The position of molecular weight marker is indicated on the left.

Figure S2. Preabsorption of anti-γ-secretase activating protein (GSAP) antibody with recombinant GSAP protein. Recombinant GSAP protein covering amino acid residues 734-854 tagged with Xpress was expressed in *Escherichia coli*, purified, gel-separated and blotted. The anti-GSAP antibody (HPA020058) was incubated at 4°C overnight with the recombinant GSAP protein, and then processed for immunohistochemistry. The panels (**a–c**) represent (**a**) Western blot of recombinant GSAP protein by using the antibody HPA020058 (lane 1) and anti-Xpress antibody (lane 2), (**b**) immunohistochemistry of the hippocampal CA3 region of Alzheimer's disease by using the non-absorbed antibody, and (**c**) immunohistochemistry of the same region by using the preabsorbed antibody.

Figure S3. Multiple sequence alignment of γ-secretase activating protein (GSAP) derived from various species. Amino acid sequences of the GSAP segment of PION of various species and pigeon of *Drosophila melanogaster* are aligned by using CLC Free Workbench version 4.5.1 (CLC Bio, Aarhus, Denmark). They are derived from the GenBank data under the accession number of *Homo sapiens* (Entrez Gene ID 54103), *Pan troglodytes* (472424), *Bos taurus* (615147), *Canis lupus familiaris* (475903), *Mus musclus* (212167), *Rattus norvegiucus* (311984), *Gallus gallus* (417724), *Danio rerio* (100151358) and *Drosophila melanogaster* (35200).

Table S1. The cases examined in the present study.

Please note: Wiley-Blackwell are not responsible for the content or functionality of any supporting materials supplied by the authors. Any queries (other than missing material) should be directed to the corresponding author for the article.

Received 8 February 2011
Accepted after revision 27 June 2011
Published online Article Accepted on 30 June 2011

Experimental Neurology 235 (2012) 436–446

Contents lists available at SciVerse ScienceDirect

Experimental Neurology

journal homepage: www.elsevier.com/locate/yexnr

Review

Molecular network of microRNA targets in Alzheimer's disease brains

Jun-ichi Satoh *

Department of Bioinformatics and Molecular Neuropathology, Meiji Pharmaceutical University, 2-522-1 Noshio, Kiyose, Tokyo 204-8588, Japan

ARTICLE INFO

Article history:
Received 20 April 2011
Revised 24 August 2011
Accepted 4 September 2011
Available online 16 September 2011

Keywords:
Alzheimer's disease
Cell cycle
KEGG
KeyMolnet
MicroRNA
MiRTarBase

ABSTRACT

MicroRNAs (miRNAs) are a group of small noncoding RNAs that regulate translational repression of target mRNAs. The vast majority of presently identified miRNAs are expressed in the brain where they fine-tune the expression of a wide range of target molecules essential for neuronal and glial development, differentiation, proliferation, apoptosis and metabolism. Aberrant expression and dysfunction of brain-enriched miRNAs induce development of neurodegenerative diseases, such as Alzheimer's disease (AD) and Parkinson's disease (PD). Because a single miRNA concurrently downregulates hundreds of target mRNAs, the set of miRNA target genes coregulated by an individual miRNA generally constitutes the biologically integrated network of functionally associated molecules. Recent advances in systems biology enable us to characterize the global molecular network of experimentally validated targets for individual miRNAs by using pathway analysis tools of bioinformatics endowed with comprehensive knowledgebase. This review is conducted to summarize accumulating studies focused on aberrant miRNA expression in AD brains, and to propose the systems biological view that abnormal regulation of cell cycle progression as a result of deregulation of miRNA target networks plays a central role in the pathogenesis of AD.

Contents

Introduction

MicroRNAs (miRNAs) constitute a class of endogenous small noncoding RNAs that mediate posttranscriptional regulation of protein-coding genes by binding mainly to the 3′ untranslated region (3′ UTR) of target mRNAs, leading to translational inhibition, mRNA destabilization or degradation, depending on the degree of sequence complementarity. During their biogenesis, the primary miRNAs (pri-miRNAs) are transcribed from the intra- and inter-genic regions of the genome by RNA polymerase II, and processed by the RNase III enzyme Drosha into pre-miRNAs. After nuclear export, they are processed by RNase III enzyme Dicer into mature miRNAs consisting of approximately 22 nucleotides. Finally, a single-stranded miRNA is loaded onto the RNA-induced silencing complex (RISC), where the seed sequence located at positions 2 to 8 from the 5′ end of the miRNA plays a crucial role in recognition of the target mRNA.

At present, more than one thousand of human miRNAs are registered in miRBase Release 17 (April 2011; www.mirbase.org). A single miRNA capable of binding to numerous target mRNAs concurrently reduces production of hundreds of proteins, whereas the 3′UTR of a single mRNA is often targeted by multiple different miRNAs, providing the complexity of miRNA-regulated gene expression (Filipowicz et al., 2008; Selbach et al., 2008). Consequently, the whole human miRNA system (microRNAome) regulates greater than 60% of all protein-coding genes essential for cellular development, differentiation, proliferation, apoptosis and metabolism (Friedman et al., 2009). Approximately 70% of presently identified miRNAs are expressed in the brain in a spatially and temporally controlled manner, where they fine-tune diverse neuronal and glial functions (Fineberg et al., 2009). Actually, aberrant expression and dysfunction of brain-enriched miRNAs induce development of neurodegenerative diseases, such as Alzheimer's disease (AD) and Parkinson's disease

* Corresponding author. Fax: +81 42 495 8678.
E-mail address: satoj@my-pharm.ac.jp.

0014-4886/$ – see front matter © 2011 Elsevier Inc. All rights reserved.
doi:10.1016/j.expneurol.2011.09.003

Table 1
Aberrant expression of miRNAs in AD brains.

Authors and years	Patients and brain regions	Methods for miRNA expression profiling	Aberrantly expressed miRNAs	Upregulation or downregulation	Target mRNAs characterized	Target prediction and validation	Possible pathological implications
Lukiw (2007)	5 AD patients and 5 age-matched controls; the hippocampus	Northern blot	miR-9, miR-128	Up	ND	ND	General neuropathology of AD
Lukiw et al. (2008)	23 AD patients and 23 age-matched controls; the hippocampus and the superior temporal lobe neocortex	Microarray, northern blot	miR-146a	Up	CFH	ND; knockdown of miR-146a	Sustained inflammatory responses
Wang et al. (2008)	6 AD and 6 MCI patients and 11 non-demented controls; the temporal cortex	Microarray, northern blot, ISH	miR-107	Down	BACE1	miRanda, TargetScan, PicTar; luciferase reporter assay	Increased production of Ab
Hébert et al. (2008)	5 AD patients and 5 age-matched controls; the anterior temporal cortex	Microarray, qRT-PCR	miR-29a/b-1	Down	BACE1	miRanda, TargetScan, Pictar, miRBase; luciferase reporter assay	Increased production of Ab
			miR-15a, miR-9, miR-19b	Down	BACE1	miRanda, TargetScan, Pictar, miRBase; not validated	
			let-7i, miR-15a, miR-101, miR-106b	Down	APP	miRanda, TargetScan, Pictar, miRBase; not validated	
			miR-22, miR-26b, miR-93, miR-181c, miR-210, miR-363	Down	ND	ND	
			miR-197, miR-511, miR-320	Up	ND	ND	
Cogswell et al. (2008)	15 AD patients and 12 non-demented controls; the cerebellum	qRT-PCR	miR-27a, miR-27b, miR-34a, miR-100, miR-125b, miR-381, miR-422a	Up	ND	miRanda, RNAhybrid; not validated	General neuropathology of AD
			miR-9, miR-98, miR-132, miR-146b, miR-212, miR-425	Down	ARHGAP32 for miR-132		
	15 AD patients and 12 non-demented controls; the hippocampus		miR-26a, miR-27a, miR-27b, miR-30e-5p, miR-34a, miR-92, miR-125b, miR-145, miR-200c, miR-381, miR-422a, miR-423	Up	ND		
			miR-9, miR-30c, miR-132, miR-146b, miR-210, miR-212, miR-425	Down	ARHGAP32 for miR-132		
	15 AD patients and 12 non-demented controls; the medial frontal gyrus		miR-27a, miR-27b, miR-29a, miR-29b, miR-30c, miR-30e-5p, miR-34a, miR-92, miR-100, miR-125b, miR-145, miR-148a, miR-381, miR-422a, miR-423	Up	ND		
			miR-9, miR-26a, miR-132, miR-146b, miR-200c, miR-210, miR-212, miR-425	Down	ARHGAP32 for miR-132		
Hébert et al. (2009)	19 AD patients and 11 non-demented controls; the anterior temporal cortex	qRT-PCR	miR-106b	Down	APP	miRanda, TargetScan, Pictar, miRBase; luciferase reporter assay	Increased production of Ab
Sethi and Lukiw (2009)	6 AD and 13 non-AD patients and 6 controls; the temporal lobe cortex	Microarray, northern blot	miR-9, miR-125b, miR-146a	Up	ND	ND	General neuropathology of AD
Nunez-Iglesias et al. (2010)	5 AD patients and 5 age-matched controls; the parietal lobe cortex	Microarray	miR-18b, miR-34c, miR-615, miR-629, miR-637, miR-657, miR-661, mir-09369, mir-15903, mir-44691	Nd	positively correlated with target mRNAs	miRanda, TargetScan, PicTar; not validated	General neuropathology of AD
			miR-211, miR-216, miR-325, miR-506, miR-515-3p, miR-612, miR-768-3p, mir-06164, mir-32339, mir-45496	Nd	negatively correlated with target mRNAs	miRanda, TargetScan, PicTar; not validated	

(continued on next page)

Table 1 (*continued*)

Authors and years	Patients and brain regions	Methods for miRNA expression profiling	Aberrantly expressed miRNAs	Upregulation or downregulation	Target mRNAs characterized	Target prediction and validation	Possible pathological implications
Shioya et al. (2010)	7 AD patients and 4 non-neurological controls; the frontal lobe	qRT-PCR	miR-29a	Down	NAV3	TargetScan, Pictar, miRBase; luciferase reporter assay	A putative compensatory mechanism against neurodegenerative events
Hébert et al. (2010)	8 AD patients and 10 non-demented patients; the anterior temporal cortex	qRT-PCR	miR-15a	Down	ERK1	TargetScan, miRanda; overexpression or knockdown of miR-15a, luciferase reporter assay	Hyperphosphorylation of tau
Cui et al. (2010)	36 AD patients and 30 age-matched controls; the hippocampus and the superior temporal lobe neocortex	Microarray, northern blot	miR-146a	Up	IRAK1	miRBase; knockdown of miR-146a	Sustained inflammatory responses
Faghihi et al. (2010)	35 AD patients and 35 normal elderly controls; the entorhinal cortex and the hippocampus	qRT-PCR	miR-485-5p	Down	BACE1	miRanda; luciferase reporter assay	increased production of Ab
Smith et al. (2011)	11 AD patients and 11 non-demented patients; the anterior temporal cortex	qRT-PCR	miR-124	Down	PTBP1	known target previously validated by luciferase reporter assay	Aberrant APP mRNA alternative splicing
Wang et al. (2011)	10 elderly females with various pathological stages of AD; the gray matter and the white matter of the superior and middle temporal cortex	Microarray, northern blot	miR-519e, miR-574-5p, miR-498, miR-518a-5p/miR-527, miR-525-5p, miR-300, miR-576-3p, miR-583, miR-146b-3p, miR-490-3p, miR-549, miR-516a-5p, miR-510, miR-184, miR-516b, miR-298, miR-214, miR-198, miR-451, miR-144, miR-424, let-7e miR-509-5p, miR-574-3p, miR-576-5p, miR-302e, miR-220b, miR-208a, miR-215 miR-485-3p, miR-381, miR-124, miR-34a, miR-129-5p, miR-29a, miR-143, miR-136, miR-145, miR-138, miR-129-3p, miR-128, miR-379, miR-299-5p, miR-218, miR-149, miR-135a, miR-7, miR-126, miR-411, miR-335, miR-9, miR-378, miR-488, miR-432,	Up in the gray matter (group A) Up in the white matter (group B) Down in the gray matter (group C)	ND	ND	General neuropathology of AD

miR-127-5p, miR-127-3p, miR-491-5p, miR-376c, miR-377, miR-95, miR-222, miR-29b, miR-329, miR-495, miR-551b, miR-195, miR-125b, miR-30b, miR-221, miR-139-5p, miR-487a, miR-487b, miR-107, miR-146b-5p, miR-29c, miR-30a, miR-582-5p, miR-103, miR-342-3p, miR-331-3p, miR-30c, miR-30d, miR-382, miR-22, miR-125a-5p	
miR-491-3p, miR-423-5p, miR-34b, miR-422a, miR-34c-5p, miR-584, miR-219-5p, miR-338-3p, miR-219-2-3p, miR-338-5p, miR-181a, miR-181b, let-7b, miR-151-3p, miR-197, miR-19a, miR-20a, miR-17, miR-106a, miR-32, miR-340, miR-19b, miR-21, miR-151-5p, miR-194, let-7c, miR-330-3p, miR-27b, miR-93, miR-15a, miR-339-5p, miR-193b, miR-106b, miR-16, miR-23b, miR-15b, miR-320d, miR-320b, miR-320c, miR-320a, miR-557, miR-33a, let-7a, miR-374b, miR-140-3p, miR-374a, miR-24, miR-140-5p, miR-26a, miR-513a-5p, miR-212, miR-142-5p, miR-142-3p, miR-26b, miR-520d-5p, miR-193a-3p, miR-92b, miR-330-5p, miR-186, let-7f, miR-223, miR-412, miR-185, miR-148b, miR-101, miR-99b, miR-27a, miR-589, let-7i, miR-361-3p, miR-361-5p, miR-423-3p, miR-190, miR-301a, miR-365, miR-23a, miR-363, miR-326	Down in the white matter (group D)
miR-425, miR-191, miR-519d, let-7 g, miR-98, miR-99a, miR-30e	Down in the gray matter (group E)

The table is modified from that of the recent review article with permission of reproduction (Satoh, 2010). Abbreviations: AD, Alzheimer disease; MCI, mild cognitive impairment; qRT-PCR, quantitative RT-PCR; ISH, in situ hybridization; BACE1, beta-site APP-cleaving enzyme 1; APP, amyloid precursor protein; Ab, amyloid-beta; CFH, complement factor H; NAV3, neuron navigator 3; ERK1, extracellular signal-regulated kinase 1; ARHGAP32, Rho GTPase activating protein 32 (p250GAP); IRAK1, IL-1 receptor-associated kinase-1; PTBP1, polypyrimidine tract binding protein 1; and ND, not determined.

(PD) (Harraz et al., 2011; Kocerha et al., 2009; Maes et al., 2009; Nelson et al., 2008).

Recent advances in systems biology have made major breakthroughs by illustrating the cell-wide map of complex molecular interactions with the aid of the literature-based knowledgebase of molecular pathways (Viswanathan et al., 2008). The logically arranged molecular networks construct the whole system characterized by robustness that maintains the proper function of the system in the face of genetic and environmental perturbations (Kitano, 2007). In the scale-free molecular network, targeted disruption of several critical components designated hubs, on which the biologically important molecular interactions concentrate, efficiently disturbs the whole cellular function by destabilizing the network (Albert et al., 2000). From the point of view of the molecular network constructed by target genes for a particular miRNA, the identification and characterization of the hub would help us to understand biological and pathological roles of the individual miRNA. By combining the application of the miRNA target prediction program TargetScan and the Human Protein Reference Database (HPRD), a recent study investigated the global human microRNA-regulated protein–protein interaction (PPI) network (Hsu et al., 2008). Importantly, individual miRNAs often target the hub itself within the PPI network.

AD is the most common cause of dementia worldwide, affecting the elderly population, characterized by the hallmark pathology of amyloid-β (Aβ) deposition, neurofibrillary tangle (NFT) formation, and extensive neuronal degeneration in the brain. Aβ is derived from the sequential cleavage of amyloid precursor protein (APP) by beta-site APP-cleaving enzyme 1 (BACE1) and the γ-secretase complex. Although the precise pathological mechanisms underlying AD remain largely unknown, accumulating evidence indicates that aberrant regulation of miRNA-dependent gene expression is closely associated with molecular events responsible for Aβ production, NFT formation, and neurodegeneration (Hébert et al., 2008, 2010; Wang et al., 2008, 2011). The aim of the present study is to review recent studies focused on aberrant miRNA expression in AD brains, and to propose the systems biological view that deregulation of miRNA target networks plays a central role in the pathogenesis of AD.

Aberrant miRNA expression in AD brains

Increasing evidence indicates that deregulation of miRNA expression plays a key role in AD pathogenesis, as a recent review indicated (Table 1 modified from Satoh, 2010). The pioneering work identified upregulated expression of miR-9 and miR-128 in the hippocampus of AD brains by using a nylon membrane-bound DNA array (Lukiw, 2007). More recently, the same group showed that the levels of expression of miR-146a are elevated in the hippocampus and the superior temporal cortex of AD patients (Lukiw et al., 2008). Importantly, nuclear factor-kappa B (NF-κB), a transcription factor indispensable for diverse immune responses, regulates the expression of miR-146a that targets complement factor H (CFH) and IL-1 receptor-associated kinase-1 (IRAK1), leading to sustained inflammation in AD brains where the expression of NF-κB is also upregulated (Cui et al., 2010; Lukiw et al., 2008). Furthermore, they clarified the limited stability of brain-enriched miRNAs composed of a high content of AU and UA dinucleotides (Sethi and Lukiw, 2009).

A different group showed that miR-107 targets BACE1, a rate-limiting enzyme for Aβ production (Wang et al., 2008). By analyzing a miRNA microarray, they found that miR-107 levels are substantially reduced in the temporal cortex not only of AD but also of the patients affected with mild cognitive impairment (MCI), indicating that downregulation of miR-107 begins at the very early stage of AD. More recently, they validated a negative correlation between miR-107 levels and the amounts of neuritic plaques and NFTs in the temporal cortex of AD patients by quantitative RT-PCR (qRT-PCR) (Nelson and Wang, 2010). The levels of miR-107 and miR-103, both of which target the actin-binding protein cofilin, are reduced in the brains of Tg19959 mice overexpressing human APP carrying the KM670/671NL and V717F familial AD mutations (Yao et al., 2010). These observations are responsible for formation of rod-like aggregates of cofilin in brains of a transgenic mouse model of AD.

By using a miRNA microarray, a previous study identified reduced expression of the miR-29a/b-1 cluster, inversely correlated with BACE1 protein levels, in the anterior temporal cortex of AD patients (Hébert et al., 2008). The miRNA target database search predicted the presence of binding sites in the human BACE1 mRNA 3′UTR for miR-9, 15a, 19b, and 29a/b-1 and in the human APP mRNA 3′UTR for let-7, miR-15a, 101, and 106b, all of which are downregulated in AD brains. Actually, the introduction of pre-miR-29 reduces secretion of Aβ from HEK293 cells stably expressing the APP Swedish (APPswe) mutation (Hébert et al., 2008). Later, they identified reduced expression of miR-106b that targets APP in the anterior temporal cortex of AD patients (Hébert et al., 2009).

The levels of miR-298 and miR-328, both of which target mouse BACE1, are reduced in the hippocampus of aged APPswe/PS1(A246E) transgenic mice (Boissonneault et al., 2009). In contrast, the levels of a noncoding BACE1-antisense (BACE1-AS) RNA that enhances BACE1 mRNA stability are elevated in the brains of Tg19959 APP transgenic mice (Faghihi et al., 2008). BACE1-AS masks the miR-485-5p binding site located within the open-reading frame of BACE1 mRNA, and thereby inhibits miR-485-5p-mediated repression of BACE1 mRNA translation (Faghihi et al., 2010). Actually, the levels of expression of miR-485-5p are reduced but those of BACE1-AS are elevated in the entorhinal cortex and the hippocampus of AD patients. In cultured rat hippocampal neurons, a brain-enriched microRNA miR-101 acts as a negative regulator of APP expression by binding to the APP 3′UTR (Vilardo et al., 2010).

All of these observations suggest the concept that abnormal repression of a battery of miRNAs accelerates Aβ production via overexpression of BACE1, the enzyme and/or APP, the substrate in AD brains. However, the genetic variability of miRNA-binding sites in both BACE1 and APP mRNA 3′UTRs does not confer a risk factor for development of AD (Bettens et al., 2009). It sounds reasonable, because miRNAs in general induce translational inhibition without requiring the perfect match of binding sequences in target mRNAs. It is worthy to note that a neuron-specific microRNA miR-124, downregulated in the anterior temporal cortex of AD brains, targets polypyrimidine tract binding protein 1 (PTBP1), a global repressor of alternative pre-mRNA splicing (Smith et al., 2011). Upregulation of PTBP1 induces the inclusion of APP exons 7 and 8, suggesting a novel role of miRNAs in neuronal splicing regulation of APP.

By qRT-PCR and luciferase reporter assay, we found that miR-29a, whose levels are decreased in the frontal cortex of AD brains, targets neuron navigator 3 (NAV3) (Shioya et al., 2010). NAV3 immunoreactivity was greatly enhanced in NFT-bearing pyramidal neurons in the cerebral cortex of AD brains. Although the precise biological function of the human NAV3 protein remains unknown, the *Caenorhabditis elegans* homolog regulates axon guidance (Maes et al., 2002), suggesting that our findings reflect a neuronal compensatory response against NFT-generating neurodegenerative events. The conditional deletion of Dicer, a master regulator of miRNA processing, induces neurodegeneration accompanied by hyperphosphorylation of tau in the adult mouse forebrain and the hippocampus (Hébert et al., 2010). They identified extracellular signal-regulated kinase 1 (ERK1) regulated by the miR-15 family as a candidate kinase responsible for tau phosphorylation. The levels of miR-15a are substantially reduced in AD brains.

By qRT-PCR, a previous study characterized miRNA expression profiles of the brain and cerebrospinal fluid (CSF) samples isolated from AD patients and non-demented controls (Cogswell et al., 2008). Among a panel of miRNAs either upregulated or downregulated in the hippocampus, the medial frontal cortex, and the cerebellum of AD patients, they identified a close relationship between upregulated miRNAs and metabolic pathways, including insulin signaling, glycolysis, and

glycogen metabolism. Furthermore, they found that the levels of all miR-30 family members are elevated in CSF samples of AD patients. Because circulating miRNAs in the plasma serve as a biomarker for diagnosis and prediction of prognosis of human cancers (Mitchell et al., 2008), the identification of AD-specific miRNAs in the serum and the CSF would be a worthwhile project in the future.

By combining microarray-based miRNA expression profiling and genome-wide transcriptome analysis of the brains of AD patients and age-matched controls, a recent study showed that the levels of several miRNAs are not only negatively but also positively correlated with those of potential target mRNAs (Nunez-Iglesias et al., 2010). The expression of miR-211 shows a negative correlation with mRNA levels of BACE1, RAB43, LMNA, MAP2K7, and TADA2L, whereas the expression of mir-44691 exhibits a positive correlation with mRNA levels of CYR61, CASR, POU3F2, GGPR68, DPF3, STK38, and BCL2L2 in AD brains. Although a previous study showed that certain miRNAs exceptionally activate transcription and translation of targets (Vasudevan et al., 2007), the direct interaction between mir-44691 and their targets requires further investigation and validation.

Thus, different studies identified aberrant expression of distinct miRNAs in AD brains. This variability is mostly attributable to disease-specific and nonspecific interindividual differences, including differences in age, sex, genetic background, the brain region, the pathological stage, and the postmortem interval (PMI), because most studies include fairy limited numbers of patients' samples and controls, which are often complicated by variable confounding factors (Table 1). Importantly, distinct populations of neurons in different cerebral cortical layers express a discrete set of miRNAs in the human transentorhinal cortex (Nelson et al., 2010).

MicroRNA target networks suggest the involvement of deregulation of cell cycle progression in AD pathogenesis

Because a single miRNA concurrently downregulates hundreds of target mRNAs, the set of miRNA target genes coregulated by an individual miRNA generally constitutes the biologically integrated network of functionally associated molecules (Hsu et al., 2008; Satoh and Tabunoki, 2011). Even small changes in the expression level of a single miRNA could affect a wide range of signaling pathways involved in diverse biological functions. From this point of view, the characterization of a global picture of miRNA target networks would promote us to understand miRNA-mediated molecular mechanisms underlying AD.

To identify biologically relevant molecular networks from the large-scale data, we could analyze them by using a battery of pathway analysis tools of bioinformatics endowed with comprehensive knowledgebase, such as Kyoto Encyclopedia of Genes and Genomes (KEGG) (Kanehisa et al., 2010; www.kegg.jp), Ingenuity Pathways Analysis (IPA) (Ingenuity Systems; www.ingenuity.com), and KeyMolnet (Institute of Medicinal Molecular Design; www.immd.co.jp). KEGG is a public database, while both IPA and KeyMolnet are commercial ones. KEGG includes manually curated reference pathways that cover a wide range of metabolic, genetic, environmental, and cellular processes, and human diseases. Currently, KEGG contains 134,511 distinct pathways generated from 391 reference pathways.

IPA is a knowledgebase that contains approximately 2,270,000 biological and chemical interactions and functional annotations with definite scientific evidence, curated by expert biologists. By uploading the list of Gene IDs and expression values, the network-generation algorithm identifies focused genes integrated in a global molecular network. IPA calculates the score p-value that reflects the statistical significance of association between the genes and the networks by the Fisher's exact test.

KeyMolnet contains knowledge-based contents on 131,000 relationships among human genes and proteins, small molecules, diseases, pathways and drugs, curated by expert biologists (Satoh et al., 2009). They are categorized into the core contents collected from selected review articles with the highest reliability or the secondary contents

Table 2
Gene ontology terms of target genes for miRNAs downregulated in AD brains.

Rank	GO term	The number of genes in the term	Bonferroni corrected p-value
1	GO:0042127 – regulation of cell proliferation	126	3.37E-25
2	GO:0043067 – regulation of programmed cell death	119	4.03E-20
3	GO:0010941 – regulation of cell death	119	5.55E-20
4	GO:0042981 – regulation of apoptosis	117	1.88E-19
5	GO:0043069 – negative regulation of programmed cell death	69	1.88E-16
6	GO:0051094 – positive regulation of developmental process	60	2.01E-16
7	GO:0060548 – negative regulation of cell death	69	2.20E-16
8	GO:0045597 – positive regulation of cell differentiation	54	2.80E-16
9	GO:0043066 – negative regulation of apoptosis	68	3.75E-16
10	GO:0010604 – positive regulation of macromolecule metabolic process	114	1.00E-15
11	GO:0008284 – positive regulation of cell proliferation	73	2.13E-15
12	GO:0051726 – regulation of cell cycle	61	4.12E-13
13	GO:0012501 – programmed cell death	87	8.24E-13
14	GO:0031328 – positive regulation of cellular biosynthetic process	93	1.24E-12
15	GO:0006357 – regulation of transcription from RNA polymerase II promoter	96	2.47E-12
16	GO:0009891 – positive regulation of biosynthetic process	93	3.71E-12
17	GO:0010033 – response to organic substance	95	4.53E-12
18	GO:0051174 – regulation of phosphorus metabolic process	74	5.36E-12
19	GO:0019220 – regulation of phosphate metabolic process	74	5.36E-12
20	GO:0042325 – regulation of phosphorylation	72	7.00E-12

The list of 852 target genes for the set of miRNAs downregulated in AD brains was imported into the Functional Annotation tool of DAVID. The top 20 GO terms showing a significant association with target genes are listed with rank, GO term, the number of genes in the term, and p-value following Bonferroni correction.

Table 3
KEGG pathways of target genes for miRNAs downregulated in AD brains.

Rank	KEGG pathway	The number of genes in the pathway	Bonferroni corrected p-value
1	hsa05200:Pathways in cancer	81	3.16E-21
2	hsa05220:Chronic myeloid leukemia	32	3.77E-14
3	hsa05212:Pancreatic cancer	30	7.55E-13
4	hsa05219:Bladder cancer	23	2.00E-12
5	hsa05215:Prostate cancer	32	9.63E-12
6	hsa05222:Small cell lung cancer	28	3.81E-09
7	hsa05210:Colorectal cancer	27	2.35E-08
8	hsa05223:Non-small cell lung cancer	21	9.28E-08
9	hsa05218:Melanoma	24	1.02E-07
10	hsa04110:Cell cycle	32	1.92E-07
11	hsa04510:Focal adhesion	42	2.35E-07
12	hsa04012:ErbB signaling pathway	26	3.12E-07
13	hsa05214:Glioma	22	3.23E-07
14	hsa05213:Endometrial cancer	20	3.32E-07
15	hsa05211:Renal cell carcinoma	21	1.52E-05
16	hsa04115:p53 signaling pathway	20	4.75E-05
17	hsa05221:Acute myeloid leukemia	18	9.63E-05
18	hsa04010:MAPK signaling pathway	43	3.40E-04
19	hsa04914:Progesterone-mediated oocyte maturation	21	5.61E-04
20	hsa04350:TGF-beta signaling pathway	21	6.79E-04

The list of 852 target genes for the set of miRNAs downregulated in AD brains was imported into the Functional Annotation tool of DAVID. The top 20 KEGG pathways showing a significant association with target genes are listed with rank, KEGG pathway, the number of genes in the pathway, and p-value following Bonferroni correction. The molecular pathway entitled "hsa04110:Cell cycle" (Rank 10) is illustrated in Fig. 1.

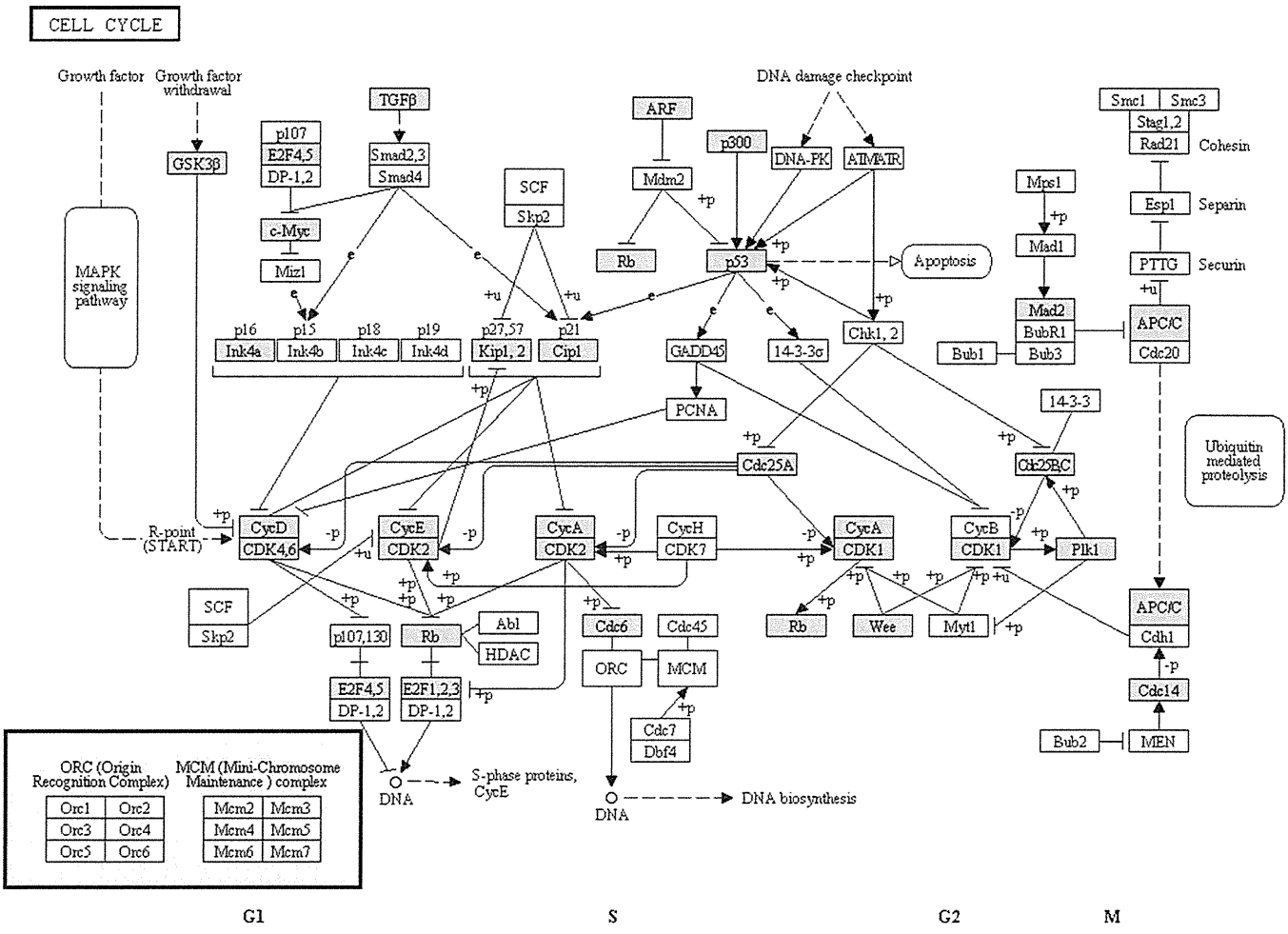

Fig. 1. Target genes for miRNAs downregulated in AD brains are located in the cell cycle pathway of KEGG. The list of 852 target genes for the set of miRNAs downregulated in AD brains (Supplementary Table 1) was imported into the Functional Annotation tool of DAVID. Among the top 20 KEGG pathways showing a significant association with target genes, the molecular pathway entitled "hsa04110:Cell cycle" (Rank 10 in Table 3) is illustrated. Target genes highlighted by pink are potentially upregulated in AD brains.

extracted from abstracts of PubMed and HPRD. By uploading the list of Gene IDs, KeyMolnet automatically provides corresponding molecules and a minimum set of intervening molecules as a node on networks. The "neighboring" network-search algorithm selected one or more molecules as starting points to generate the network of all kinds of molecular interactions around starting molecules, including direct activation/inactivation, transcriptional activation/repression, and the complex formation within the designated number of paths from starting points. The generated network was compared side by side with 443 human canonical pathways of the KeyMolnet library. The algorithm counting the number of overlapping molecular relations between the extracted network and the canonical pathway makes it possible to identify the canonical pathway showing the most significant contribution to the extracted network. The significance in the similarity between both is scored following the formula, where O = the number of overlapping molecular relations between the extracted network and the canonical pathway, V = the number of molecular relations located in the extracted network, C = the number of molecular relations located in the canonical pathway, T = the number of total molecular relations, and the X = the sigma variable that defines coincidence.

$$\text{Score} = -\log_2(\text{Score(p)}) \qquad \text{Score(p)} = \sum_{x=0}^{\text{Min(C,V)}} f(x) \qquad f(x) = {}_{C}C_{X} \cdot {}_{T-C}C_{V-X} / {}_{T}C_{V}.$$

In the present study, we attempted to characterize the networks of target genes for a battery of miRNAs aberrantly expressed in AD brains. For this purpose, we have focused on the currently available most comprehensive dataset of miRNA expression profiling of AD brains (Wang et al., 2011) (Table 1). This includes expression profiles of miRNAs isolated separately from the gray matter and the white matter of the superior and middle temporal cerebral cortex. All samples were taken within 4 h at PMI and processed for the rigid control of RNA quality. The samples were derived from control subjects with no AD pathology and the patients with the early AD pathology, evaluated by the density of diffuse plaques, neuritic plaques, and NFTs. Hierarchical clustering of expression profiles categorized AD-relevant 171 miRNAs into five groups tentatively named A to E, presenting with similar expression patterns within the group, either upregulated or downregulated in the gray matter or in the white matter of AD brains (Wang et al., 2011) (Table 1). Because the white matter is enriched in neuronal axons in which certain miRNAs are transported (Schratt et al., 2006), the white matter-enriched fraction does not exclude the inclusion of neuron-specific miRNAs. For simplicity, we combined the data of the white matter and the gray matter fractions, and separated them into two categories, such as the set of upregulated miRNAs consisting of groups A and B and the set of downregulated miRNAs consisting of groups C, D, and E.

Recently, various bioinformatics programs armed with distinct algorithms have been established for the in silico prediction of miRNA

Table 4
IPA functional networks of target genes for miRNAs downregulated in AD brains.

Rank	IPA functional network	Molecules in the network	Fisher's test p-value
1	Cancer, dermatological diseases and conditions, cellular growth and proliferation	Ap1, BCL2, CAV1, CEBPA, CEP63, COMMD9, CTGF, ETS1, FGF2, GLI1, HRAS, Ige, JUN, KRAS, NFKB1, NIPAL2, Nos, OSBPL8, P38 MAPK, PAPSS2, PLAG1, PTGFRN, PTGS2, PXDN, SERBP1, SIGMAR1, SOX9, SP1, SP3, SPP1, SQSTM1, VDR, VEGFA, VIM, WT1	1.00E-43
2	Organ development, cellular development, nervous system development and function	ACTR8, ACVR1, ACVR1B, ADSS, Alp, ANKRD27, BMP, BMP7, BMPR2, BMPR1B, COL1A2, CSHL1, CTDSP1, CTDSP2, DLL1, GSK3B, HES1, ID2, ID3, IGF2BP1, KLF4, MIR24 (human), Notch, NOTCH1, NOTCH2, Pro-inflammatory Cytokine, RAB21, Smad, SMAD1, SMAD5, SOX2, TGFBR1, TGFBR2, UHMK1, ZBED3	1.00E-38
3	Gene expression, cell cycle, DNA replication, recombination, and repair	ASXL2, BMI1, BTG2, CBX7, CDCA4, CDK2-CyclinE, DHFR, DNA (cytosine-5-)-methyltransferase, DNMT1, DNMT3A, DNMT3B, E2F2, E2F3, E2F5, E2F6, ERK, EZH2, Gap, HELLS, JARID2, MIR101, MIR125B (human), MIR26A (human), MYT1, PHB, PHF19, RING1, SGPL1, SNAI2, SPRED1, TDG, Thymidine Kinase, TYMS, UHRF1, ZNF238	1.00E-34
4	Cell cycle, connective tissue development and function, cellular growth and proliferation	ARID4B, ARL2, AURKB, BRCA1, CA12, CCDC99, CCNT2, CDCA7L, CDKN2A, DKK1, DRAM1, E2F1, Ep300/Pcaf, ERH, EYA4, FAM3C, GTF2H1, Histone h4, Holo RNA polymerase II, P-TEFb, PERP, PRMT5, Rb, RNA polymerase II, RPA, RRP8, SIRT1, TAF9B, TARBP1, TMED2, TMED7, TMED10, TMEM43, TP53, TP53INP1	1.00E-33
5	Lipid metabolism, molecular transport, small molecule biochemistry	26s Proteasome, Alpha tubulin, ARIH2, ATXN1, CDC34, CDKAL1, FADS2, HARS, HMG CoA synthase, Ikb, IKK (complex), LASS2, MAN2A1, MAPK1IP1L, MDM4, NOVA1, ODZ2, PECI, PFK, PTEN, RAD23B, SLC25A1, SLC25A22, SNCA, SOX4, SRSF10, TUBB6, UBE2, Ube3, UBE2I, UBE2Q1, UBE2S, UBE2V1, Ubiquitin, UGP2	1.00E-31
6	Lipid metabolism, small molecule biochemistry, cell signaling	ACAA2, acetyl-CoA C-acyltransferase, ANXA8/ANXA8L1, Arginase, BACE1, BNIP3L, CASP6, CASP3/6/7, Cytokeratin, Fgfr, FMOD, FNDC3B, HADH, HADHB, Hspg, IMPDH1, Lamin, LMNB1, MBNL2, Mediator, Mhc class ii, MPHOSPH9, MTRR, NAT6, NUCB1, PGRMC1, PGRMC2, PNP, RBMS1, RPS7, SLC35A1, Tenascin, TGFB1, UGDH, VPS39	1.00E-30
7	Cell cycle, cell death, cancer	ABHD5, ADIPOR2, AP2A1, APC, APP, CDKN1A, CLDND1, ELMOD2, EP300, ERBB2, GLCCI1, Hemoglobin, HIF1A, HISTONE, Histone h3, HNRNPK, IL1, Insulin, LAMB3, LRRC8C, MAN1A1, MYC, Ndpk, NR3C1, PPARA, PPARG, RAB34, RAD51C, RB1, RELA, ROCK2, SLC38A1, SLC7A11, TNFRSF21, UTP15	1.00E-30
8	Cell-to-cell signaling and interaction, cellular growth and proliferation, connective tissue development and function	ATP2A2, BRAP, CCND1, CCND2, CCND3, CDCA7, CENPJ, CTNNBIP1, Cyclin D1/cdk4, EIF4A, EIF4A1, EIF4E, Eif4ebp, EIF4EBP1, Eif4g, Gm-csf, IDH1, IGF2, IGF2R, JAK2, KAT2B, LIF, MTPN, NR4A2, p70 S6k, Pdgf (complex), PDGF BB, PMS1, SKAP2, STAT, STAT5A, STAT5a/b, TGFB3, TUSC2, UAP1	1.00E-29
9	Cellular growth and proliferation, tumor morphology, cellular development	Adaptor protein 1, AFF1, AP1M2, Camk, CAMK2G, Creb, CREB1, DNAJ, DNAJB4, DNAJB11, DNAJC1, DNAJC27, Gi-coupled receptor, Glutathione peroxidase, GSTM4, Hdac, HDAC4, HLA-G, HOXA11, HSP, Hsp70, Hsp90, Hsp22/Hsp40/Hsp90, HSP90B1, HSPA1A/HSPA1B, HSPB6, INO80C, MHC Class II (complex), MLL, MLLT1, OPRM1, PDHA2, SLC16A1, SOD2, TFRC	1.00E-26
10	Cell death, cellular growth and proliferation, connective tissue development and function	BIRC3, CASP3, CASP7, Caspase, CCL2, CCL4, CD8, CDC6, CHEMOKINE, COX4I1, DFF, DFFA, DFFB, DR4/5, DUB, HERC6, Hsp27, IFIT5, Ifn gamma, IL-1R, IL1RN, Interferon alpha, LDL, MCL1, NAIP, NEDD4, PANX1, PDCD6IP, PLSCR3, RFFL, TNFRSF10B, TNFSF10, USP18, USP48, USP49	1.00E-26

The list of 852 target genes for the set of miRNAs downregulated in AD brains was uploaded into IPA. The top 10 functional networks showing a significant association with target genes are listed with rank, IPA functional network, molecules in the network, and p-value by the Fisher's Exact test. The molecular network entitled "Cell cycle, connective tissue development and function, cellular growth and proliferation" (Rank 4) is illustrated in Fig. 2.

target genes, such as TargetScan 5.1 (www.targetscan.org), PicTar (pictar.mdc-berlin.de), miRanda (www.microrna.org), MicroCosm (www.ebi.ac.uk/enright-srv/microcosm/htdocs/targets/v5), and DianamicroT 3.0 (diana.cslab.ece.ntua.gr/microT). However, the miRNA target prediction by these programs is often hampered by detection of numerous false positive targets. To avoid this problem, we explored the targets for AD-relevant 171 miRNAs of Wang's dataset by using the miRTarBase (mirtarbase.mbc.nctu.edu.tw), the recently established largest collection of more than 3500 manually curated miRNA-target interactions from 985 articles, all of which are experimentally validated by luciferase reporter assay, western blot, qRT-PCR, microarray experiments with overexpression or knockdown of miRNAs, or pulsed stable isotope labeling with amino acids in culture (pSILAC) experiments (Hsu et al., 2011) (Supplementary Tables 1 and 2).

Although experimentally validated targets represent a source of reliable candidates, it is worthless when they are not expressed in the human brain. Therefore, we verified the expression of target genes in the human brain at mRNA levels by analyzing them on UniGene (www.ncbi.nlm.nih.gov/unigene), an organized view of the transcriptome that semi-quantitatively exhibits the expression sequence tag (EST) profile as the number of transcripts per million (TPM). After omitting the genes undetectable in the human brain, we identified 852 non-redundant target genes for the set of miRNAs downregulated in AD brains (Supplementary Table 1). We also found 39 non-redundant target genes for the set of miRNAs upregulated in AD brains (Supplementary Table 2). Since the former greatly outnumbered the latter, thereafter, we have focused on molecular networks of 852 theoretically upregulated targets for the set of downregulated miRNAs in AD brains.

Next, we investigated molecular networks of 852 genes by searching them on the Database for Annotation, Visualization and Integrated Discovery (DAVID) (david.abcc.ncifcrf.gov), which automatically outputs the results from KEGG pathway analysis (Huang et al., 2009). When Entrez Gene IDs of 852 genes were imported into the

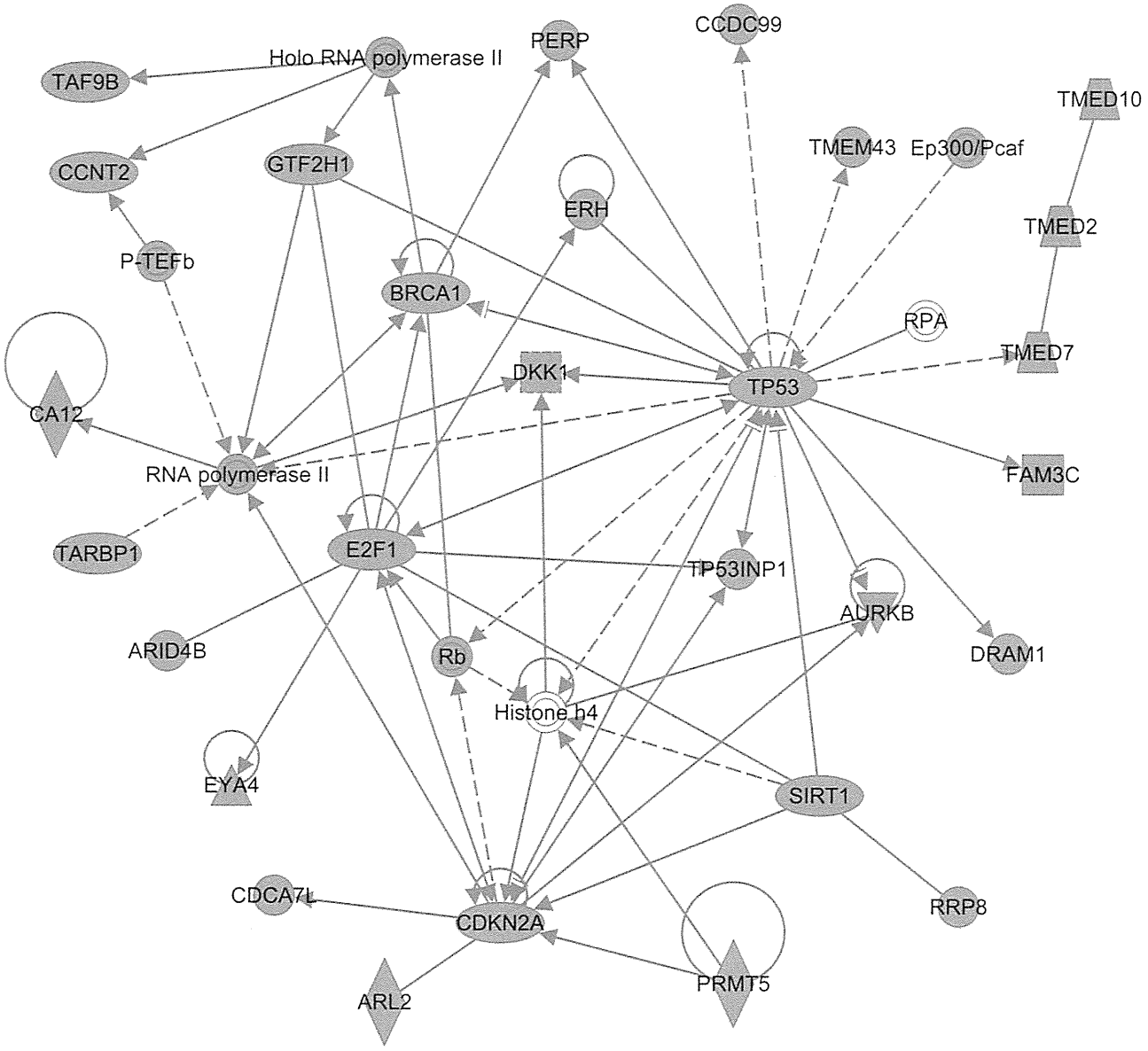

Fig. 2. Target genes for miRNAs downregulated in AD brains are located in the cell cycle-related network of IPA. The list of 852 target genes for the set of miRNAs downregulated in AD brains (Supplementary Table 1) was imported into IPA. Among the top 10 functional networks showing a significant association with target genes, the molecular network entitled "Cell cycle, connective tissue development and function, cellular growth and proliferation" (Rank 4 in Table 4) is illustrated. Target genes highlighted by red are potentially upregulated in AD brains.

Functional Annotation tool of DAVID, it identified a statistically significant association of the genes with several functional annotation categories (Table 2) and KEGG pathways (Table 3). The set of 852 genes showed a significant association with gene ontology (GO) terms related to regulation of cell proliferation, cell death, apoptosis, and cell cycle (Table 2). They also constructed KEGG pathways related to various types of cancers, cell cycle, focal adhesion, and signaling pathways of ErbB, p53, MAPK and TGF-beta (Table 3). Collectively, we concluded that a battery of cell cycle regulators, including cyclins, cyclin-dependent kinases (CDKs), cyclin-dependent kinase inhibitors (CDKIs), retinoblastoma protein (Rb), E2F family proteins, and p53, are highly enriched in both GO terms and KEGG pathways (Fig. 1).

Then, we validated the crucial involvement of cell cycle pathway in the molecular network of 852 target genes by uploading them into IPA and KeyMolnet. IPA suggested that these genes show a significant association with functional networks of cancer, cell growth, proliferation, development, and death, and cell cycle (Table 4). Again, major members of cell cycle regulators, including Rb, E2F1, and p53, are clustered in these networks (Fig. 2). KeyMolnet, based on the neighboring network-search algorithm, extracted a highly complex network composed of 3428 molecules and 6837 molecular relations, exhibiting a significant association with transcriptional regulation by a battery of transcription factors, such as Rb/E2F, cAMP responsive element binding protein (CREB), glucocorticoid receptor (GR), vitamin D receptor (VDR), NF-κB, hypoxia inducible factor (HIF), p53, and AP-1 (Fig. 3) (Table 5). Although the molecular pathways and networks illustrated by three different programs KEGG, IPA, and KeyMolnet armed with distinct computational algorithms do not perfectly merge each other, all the results supported the working hypothesis that the set of miRNAs downregulated in AD brains induces abnormal regulation of cell cycle progression via synchronous upregulation of multiple cell cycle regulators.

The cell cycle progression is positively and negatively regulated by the complex checkpoint mechanism. Increasing evidence convincingly shows aberrant expression of cell cycle regulators in the hippocampus, the basal forebrain, and the cerebral cortex of AD brains. They

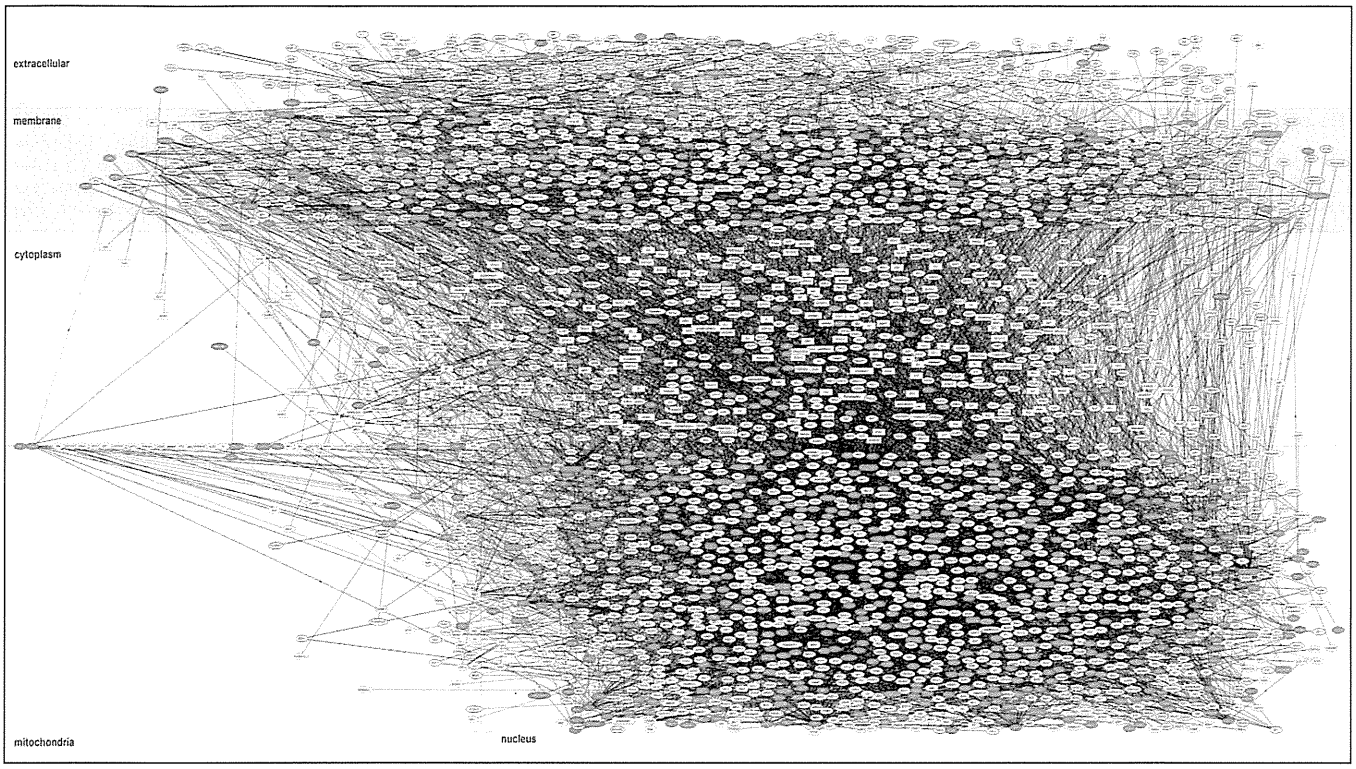

Fig. 3. KeyMolnet illustrates the highly complex molecular network of target genes for miRNAs downregulated in AD brains. The list of 852 target genes for the set of miRNAs downregulated in AD brains (Supplementary Table 1) was imported into KeyMolnet. The highly complex molecular network extracted by the neighboring network-search algorithm, composed of 3428 molecules and 6837 molecular relations, suggested the most significant relationship with the canonical pathway entitled "Transcriptional regulation by Rb/E2F" (Rank 1, Table 5). Target genes highlighted by red are potentially upregulated in AD brains.

include cyclins A, B, D, and E, along with CDKs and CDKIs of both the Cip/Kip and Ink4 families (Busser et al., 1998; McShea et al., 1997; Yang et al., 2003). The abnormal reentry into the cell cycle is an early event in neurons of AD brains stimulated by oxidative stress, which precedes Aβ deposition and NFT formation, and is potentially deleterious for terminally differentiated neurons, serving as a direct cause of neuronal apoptosis and degeneration (Bonda et al., 2010). The hypophosphorylated Rb protein interacts with the E2F family transcription factors E2F1, E2F2, and E2F3, and activates the expression of the genes pivotal for cell cycle progression, whereas the Rb protein, hyperphosphorylated by cyclin D1–CDK4 and cyclin E1–CDK2 complexes, releases E2Fs, and represses the expression of cell cycle genes (Swiss and Casaccia, 2010). Thus, the Rb/E2F pathway constitutes a molecular switch deciding either progression or arrest of the cell cycle. We found that RB1 is an experimentally validated target for miR-23b, 26a, 106a, 106b, 124a and 335, while E2F1 is a target for miR-17, 20a, 21, 23b, 93, 98, 106a, 106b, 223 and 330, E2F2 for miR-21, 24 and 98, and E2F3 for miR-34a, 34c and 195 (Supplementary Table 3). Thus, it is evident that E2F1 serves as one of hub molecules that play a central role in the cell cycle pathway. All of these miRNAs are downregulated in AD brains in the dataset of Wang et al. (Table 1), suggesting the logical hypothesis that the levels of expression of Rb and E2F proteins are abnormally elevated in AD brains (Figs. 1 and 2). Most importantly, aberrant expression of Rb protein and E2F1 is actually identified in neurons and glia cells in the frontal cortex of AD brains, where the Rb protein is hyperphosphorylated (Ranganathan et al., 2001).

In conclusion, we identified 852 experimentally validated target genes for the set of miRNAs downregulated in AD brains by searching them on the miRTarBase and UniGene. The molecular network analysis of 852 target genes by using three distinct pathway analysis tools of bioinformatics KEGG, IPA, and KeyMolnet proposed the system biological view that aberrant expression of cell cycle regulators might serve as a direct cause of neurodegeneration in AD brains.

Supplementary materials related to this article can be found online at doi:10.1016/j.expneurol.2011.09.003.

Table 5
KeyMolnet pathways of target genes for miRNAs downregulated in AD brains.

Rank	KeyMolnet pathway	Score	Score p-value
1	Transcriptional regulation by Rb/E2F	882.46	2.25E-266
2	Transcriptional regulation by CREB	688.612	5.10E-208
3	Integrin family	630.668	1.41E-190
4	Transcriptional regulation by GR	508.344	9.40E-154
5	Transcriptional regulation by VDR	497.189	2.14E-150
6	Transcriptional regulation by NF-kB	495.71	5.98E-150
7	Transcriptional regulation by HIF	488.203	1.09E-147
8	TGF-beta family signaling pathway	387.147	2.87E-117
9	Transcriptional regulation by p53	386.348	4.98E-117
10	Transcriptional regulation by AP-1	367.719	2.02E-111

The list of 852 target genes for the set of miRNAs downregulated in AD brains was uploaded into KeyMolnet. It extracted a highly complex network composed of 3428 molecules and 6837 molecular relations, as illustrated in Fig. 3. The top 10 KeyMolnet pathways showing a significant association with target genes are listed with rank, KeyMolnet pathway, score, and p-value of the score. Abbreviations: Rb, retinoblastoma; CREB, cAMP responsive element binding protein; GR, glucocorticoid receptor; VDR, vitamin D receptor; NF-kB, nuclear factor kappa B; and HIF, hypoxia inducible factor.

Acknowledgments

This work was supported by grants from the Research on Intractable Diseases, the Ministry of Health, Labour and Welfare, Japan (H22-Nanchi-Ippan-136; H21-Nanchi-Ippan-201; H21-Nanchi-Ippan-217; H21-Kokoro-Ippan-018) and the High-Tech Research Center

Project (S0801043) and the Grant-in-Aid (C22500322), the Ministry of Education, Culture, Sports, Science and Technology (MEXT), Japan.

References

Albert, R., Jeong, H., Barabasi, A.L., 2000. Error and attack tolerance of complex networks. Nature 406, 378–382.

Bettens, K., Brouwers, N., Engelborghs, S., Van Miegroet, H., De Deyn, P.P., Theuns, J., Sleegers, K., Van Broeckhoven, C., 2009. APP and BACE1 miRNA genetic variability has no major role in risk for Alzheimer disease. Hum. Mutat. 30, 1207–1213.

Boissonneault, V., Plante, I., Rivest, S., Provost, P., 2009. MicroRNA-298 and microRNA-328 regulate expression of mouse β-amyloid precursor protein-converting enzyme 1. J. Biol. Chem. 284, 1971–1981.

Bonda, D.J., Lee, H.P., Kudo, W., Zhu, X., Smith, M.A., Lee, H.G., 2010. Pathological implications of cell cycle re-entry in Alzheimer disease. Expert Rev. Mol. Med. 12, e19.

Busser, J., Geldmacher, D.S., Herrup, K., 1998. Ectopic cell cycle proteins predict the sites of neuronal cell death in Alzheimer's disease brain. J. Neurosci. 18, 2801–2807.

Cogswell, J.P., Ward, J., Taylor, I.A., Waters, M., Shi, Y., Cannon, B., Kelnar, K., Kemppainen, J., Brown, D., Chen, C., Prinjha, R.K., Richardson, J.C., Saunders, A.M., Roses, A.D., Richards, C.A., 2008. Identification of miRNA changes in Alzheimer's disease brain and CSF yields putative biomarkers and insights into disease pathways. J. Alzheimers Dis. 14, 27–41.

Cui, J.G., Li, Y.Y., Zhao, Y., Bhattacharjee, S., Lukiw, W.J., 2010. Differential regulation of interleukin-1 receptor-associated kinase-1 (IRAK-1) and IRAK-2 by microRNA-146a and NF-κB in stressed human astroglial cells and in Alzheimer disease. J. Biol. Chem. 285, 38951–38960.

Faghihi, M.A., Modarresi, F., Khalil, A.M., Wood, D.E., Sahagan, B.G., Morgan, T.E., Finch, C.E., St Laurent III, G., Kenny, P.J., Wahlestedt, C., 2008. Expression of a noncoding RNA is elevated in Alzheimer's disease and drives rapid feed-forward regulation of β-secretase. Nat. Med. 14, 723–730.

Faghihi, M.A., Zhang, M., Huang, J., Modarresi, F., Van der Brug, M.P., Nalls, M.A., Cookson, M.R., St-Laurent III, G., Wahlestedt, C., 2010. Evidence for natural antisense transcript-mediated inhibition of microRNA function. Genome Biol. 11, R56.

Filipowicz, W., Bhattacharyya, S.N., Sonenberg, N., 2008. Mechanisms of post-transcriptional regulation by microRNAs: are the answers in sight? Nat. Rev. Genet. 9, 102–114.

Fineberg, S.K., Kosik, K.S., Davidson, B.L., 2009. MicroRNAs potentiate neural development. Neuron 64, 303–309.

Friedman, R.C., Farh, K.K., Burge, C.B., Bartel, D.P., 2009. Most mammalian mRNAs are conserved targets of microRNAs. Genome Res. 19, 92–105.

Harraz, M.M., Dawson, T.M., Dawson, V.L., 2011. MicroRNAs in Parkinson's disease. J. Chem. Neuroanat. 42, 127–130.

Hébert, S.S., Horré, K., Nicolaï, L., Papadopoulou, A.S., Mandemakers, W., Silahtaroglu, A.N., Kauppinen, S., Delacourte, A., De Strooper, B., 2008. Loss of microRNA cluster miR-29a/b-1 in sporadic Alzheimer's disease correlates with increased BACE1/beta-secretase expression. Proc. Natl. Acad. Sci. U. S. A. 105, 6415–6420.

Hébert, S.S., Horré, K., Nicolaï, L., Bergmans, B., Papadopoulou, A.S., Delacourte, A., De Strooper, B., 2009. MicroRNA regulation of Alzheimer's amyloid precursor protein expression. Neurobiol. Dis. 33, 422–428.

Hébert, S.S., Papadopoulou, A.S., Smith, P., Galas, M.C., Planel, E., Silahtaroglu, A.N., Sergeant, N., Buée, L., De Strooper, B., 2010. Genetic ablation of Dicer in adult forebrain neurons results in abnormal tau hyperphosphorylation and neurodegeneration. Hum. Mol. Genet. 19, 3959–3969.

Hsu, C.W., Juan, H.F., Huang, H.C., 2008. Characterization of microRNA-regulated protein–protein interaction network. Proteomics 8, 1975–1979.

Hsu, S.D., Lin, F.M., Wu, W.Y., Liang, C., Huang, W.C., Chan, W.L., Tsai, W.T., Chen, G.Z., Lee, C.J., Chiu, C.M., Chien, C.H., Wu, M.C., Huang, C.Y., Tsou, A.P., Huang, H.D., 2011. miRTarBase: a database curates experimentally validated microRNA-target interactions. Nucleic Acids Res. 39, D163–D169.

Huang, da W., Sherman, B.T., Lempicki, R.A., 2009. Systematic and integrative analysis of large gene lists using DAVID bioinformatics resources. Nat. Protoc. 4, 44–57.

Kanehisa, M., Goto, S., Furumichi, M., Tanabe, M., Hirakawa, M., 2010. KEGG for representation and analysis of molecular networks involving diseases and drugs. Nucleic Acids Res. 38, D355–D360.

Kitano, H., 2007. A robustness-based approach to systems-oriented drug design. Nat. Rev. Drug Discov. 6, 202–210.

Kocerha, J., Kauppinen, S., Wahlestedt, C., 2009. microRNAs in CNS disorders. Neuromolecular Med. 11, 162–172.

Lukiw, W.J., 2007. Micro-RNA speciation in fetal, adult and Alzheimer's disease hippocampus. Neuroreport 18, 297–300.

Lukiw, W.J., Zhao, Y., Cui, J.G., 2008. An NF-κB-sensitive micro RNA-146a-mediated inflammatory circuit in Alzheimer disease and in stressed human brain cells. J. Biol. Chem. 283, 31315–31322.

Maes, T., Barceló, A., Buesa, C., 2002. Neuron navigator: a human gene family with homology to unc-53, a cell guidance gene from *Caenorhabditis elegans*. Genomics 80, 21–30.

Maes, O.C., Chertkow, H.M., Wang, E., Schipper, H.M., 2009. MicroRNA: implications for Alzheimer disease and other human CNS disorders. Curr. Genomics 10, 154–168.

McShea, A., Harris, P.L., Webster, K.R., Wahl, A.F., Smith, M.A., 1997. Abnormal expression of the cell cycle regulators P16 and CDK4 in Alzheimer's disease. Am. J. Pathol. 150, 1933–1939.

Mitchell, P.S., Parkin, R.K., Kroh, E.M., Fritz, B.R., Wyman, S.K., Pogosova-Agadjanyan, E.L., Peterson, A., Noteboom, J., O'Briant, K.C., Allen, A., Lin, D.W., Urban, N., Drescher, C.W., Knudsen, B.S., Stirewalt, D.L., Gentleman, R., Vessella, R.L., Nelson, P.S., Martin, D.B., Tewari, M., 2008. Circulating microRNAs as stable blood-based markers for cancer detection. Proc. Natl. Acad. Sci. U. S. A. 105, 10513–10518.

Nelson, P.T., Wang, W.X., 2010. MiR-107 is reduced in Alzheimer's disease brain neocortex: validation study. J. Alzheimers Dis. 21, 75–79.

Nelson, P.T., Wang, W.X., Rajeev, B.W., 2008. MicroRNAs (miRNAs) in neurodegenerative diseases. Brain Pathol. 18, 130–138.

Nelson, P.T., Dimayuga, J., Wilfred, B.R., 2010. MicroRNA in situ hybridization in the human entorhinal and transentorhinal cortex. Front. Hum. Neurosci. 4, 7.

Nunez-Iglesias, J., Liu, C.C., Morgan, T.E., Finch, C.E., Zhou, X.J., 2010. Joint genome-wide profiling of miRNA and mRNA expression in Alzheimer's disease cortex reveals altered miRNA regulation. PLoS One 5, e8898.

Ranganathan, S., Scudiere, S., Bowser, R., 2001. Hyperphosphorylation of the retinoblastoma gene product and altered subcellular distribution of E2F-1 during Alzheimer's disease and amyotrophic lateral sclerosis. J. Alzheimers Dis. 3, 377–385.

Satoh, J., 2010. MicroRNAs and their therapeutic potential for human diseases: aberrant microRNA expression in Alzheimer's disease brains. J. Pharmacol. Sci. 114, 269–275.

Satoh, J., Tabunoki, H., 2011. Comprehensive analysis of human microRNA target networks. BioData Min. 4, 17.

Satoh, J., Tabunoki, H., Arima, K., 2009. Molecular network analysis suggests aberrant CREB-mediated gene regulation in the Alzheimer disease hippocampus. Dis. Markers 27, 239–252.

Schratt, G.M., Tuebing, F., Nigh, E.A., Kane, C.G., Sabatini, M.E., Kiebler, M., Greenberg, M.E., 2006. A brain-specific microRNA regulates dendritic spine development. Nature 439, 283–289.

Selbach, M., Schwanhäusser, B., Thierfelder, N., Fang, Z., Khanin, R., Rajewsky, N., 2008. Widespread changes in protein synthesis induced by microRNAs. Nature 455, 58–63.

Sethi, P., Lukiw, W.J., 2009. Micro-RNA abundance and stability in human brain: specific alterations in Alzheimer's disease temporal lobe neocortex. Neurosci. Lett. 459, 100–104.

Shioya, M., Obayashi, S., Tabunoki, H., Arima, K., Saito, Y., Ishida, T., Satoh, J., 2010. Aberrant microRNA expression in the brains of neurodegenerative diseases: miR-29a decreased in Alzheimer disease brains targets neuron navigator-3. Neuropathol. Appl. Neurobiol. 36, 320–330.

Smith, P., Al Hashimi, A., Girard, J., Delay, C., Hébert, S.S., 2011. In vivo regulation of amyloid precursor protein neuronal splicing by microRNAs. J. Neurochem. 116, 240–247.

Swiss, V.A., Casaccia, P., 2010. Cell-context specific role of the E2F/Rb pathway in development and disease. Glia 58, 377–390.

Vasudevan, S., Tong, Y., Steitz, J.A., 2007. Switching from repression to activation: microRNAs can up-regulate translation. Science 318, 1931–1934.

Vilardo, E., Barbato, C., Ciotti, M., Cogoni, C., Ruberti, F., 2010. MicroRNA-101 regulates amyloid precursor protein expression in hippocampal neurons. J. Biol. Chem. 285, 18344–18351.

Viswanathan, G.A., Seto, J., Patil, S., Nudelman, G., Sealfon, S.C., 2008. Getting started in biological pathway construction and analysis. PLoS Comput. Biol. 4, e16.

Wang, W.X., Rajeev, B.W., Stromberg, A.J., Ren, N., Tang, G., Huang, Q., Rigoutsos, I., Nelson, P.T., 2008. The expression of microRNA miR-107 decreases early in Alzheimer's disease and may accelerate disease progression through regulation of β-site amyloid precursor protein-cleaving enzyme 1. J. Neurosci. 28, 1213–1223.

Wang, W.X., Huang, Q., Hu, Y., Stromberg, A.J., Nelson, P.T., 2011. Patterns of microRNA expression in normal and early Alzheimer's disease human temporal cortex: white matter versus gray matter. Acta Neuropathol. 121, 193–205.

Yang, Y., Mufson, E.J., Herrup, K., 2003. Neuronal cell death is preceded by cell cycle events at all stages of Alzheimer's disease. J. Neurosci. 23, 2557–2563.

Yao, J., Hennessey, T., Flynt, A., Lai, E., Beal, M.F., Lin, M.T., 2010. MicroRNA-related cofilin abnormality in Alzheimer's disease. PLoS One 5, e15546.